Coral genetic structure in the Western Indian Ocean mirrors ocean circulation and thermal stress

Annie S. Guillaume [1 *], Stéphane Joost [1], Sarvanen Curpen[2], Danishta Dumur Neelayya[2], Luxmibye Harree-Somah[2], Oocheetsing Sadasing[2], Luca Saponari[3], Charlotte Dale[4], Léo Barret[5], Nina Andrews[6], Manuel Poretti[7] , Véronique Berteaux-Lecellier [8,], Gael Lecellier [9], Oliver Selmoni [10,11,12 *]

Affiliations:

1. Geospatial Molecular Epidemiology group (GEOME), Laboratory for Biological Geochemistry (LGB), Ecole Polytechnique Fédérale de Lausanne (EPFL), Station 2, CH-1015 Lausanne, CH
2. Mauritius Oceanography Institute, Albion, Rivière Noire District, MU
3. Nature Seychelles, Roche Caiman, Roche Caiman, SC
4. James Cook University, Townsville City, QLD, AU
5. Bee Ecological Consulting, Victoria, Mahé, SC
6. Marine Conservation Society Seychelles, Beau Vallon, SC
7. University of Melbourne, School of Biological Sciences, Melbourne, VIC, AU
8. EMR9001 SantEco - UMR250 ENTROPIE (IRD-CNRS-UR-UNC), Promenade Roger-Laroque, Noumea Cedex, New Caledonia, FR
9. Institut des Sciences Exactes et Appliquées (ISEA) EA7484-UNC, 145, Avenue James Cook, BP R4 98 851, Nouméa, New Caledonia, FR
10. Department of Embryology, Carnegie Institution for Science, Baltimore, MD, USA
11. Department of Plant Biology, Carnegie Institution for Science, Stanford, CA, USA
12. Department of Geography, University of Zurich, CH

* Corresponding authors:

Dr Annie S. Guillaume: annie.guillaume@alumni.epfl.ch

Dr Oliver Selmoni: oliver.selmoni@geo.uzh.ch

Abstract

Global warming and rising sea temperatures are pushing many reef-building coral species towards extinction. As thermal tolerance in corals is partially heritable, identifying genes under thermal selection is critical for targeted biodiversity management. However, it remains unclear how large breaks in connectivity (>100 km of open sea) affect the spread of adaptive alleles for different coral species in discontinuous reef networks such as the West Indian Ocean (WIO). To address this, we applied a seascape genomics approach to model (i) population connectivity and (ii) thermal adaptive potentials for two keystone coral species, *Acropora muricata* and *Pocillopora damicornis*, across the WIO. For both species, corals from the Seychelles were predominantly genetically isolated from corals in Rodrigues and Mauritius, putatively an effect of regional oceanographic barriers. Furthermore, sea currents during reproductive periods better predicted genetic connectivity than did Euclidean distances for both species, highlighting that connectivity models can serve as proxies to understand dispersal potential depending on reproductive strategies. Spatial patterns of neutral genetic variation were best explained by sea surface temperature variability and mean degree heating weeks. When used in genotype–environment association (GEA) analyses, we identified hundreds of loci under putative thermal selection from linked to known heat stress responses. In *A. muricata*, five Sacsin genes—co-chaperones of the Hsp70 heat-shock protein involved in thermal stress response—were identified, alongside genes related to immune defence, antioxidant response, signalling, and protein folding. In contrast, only the centromere protein V, involved in mitosis, was enriched in *P. damicornis*. By integrating patterns of gene flow with molecular adaptations to estimate species-specific adaptive potentials, we found that large sea distances and strong oceanographic barriers inhibit the genetic exchange of adapted genotypes across the WIO, providing valuable insights to guide local and regional biodiversity management in this region.

Keywords: Adaptive potential, Conservation management, Genotype–Environment Associations (GEA), Population connectivity, Seascape genomics, Thermal adaptation

1. Introduction

Covering less than 1% of the ocean floor, coral reefs are biodiversity hotspots hosting approximately a third of all marine species (Moberg and Folke, 1999). These dynamic ecosystems provide valuable habitat for a variety of taxa, shaping food chains and biogeochemical cycles while also providing important ecosystem services for humans, including food, medicine, coastal protection, and tourism (Costanza et al., 2014; Hughes et al., 2017a; Moberg and Folke, 1999; Roff et al., 2016). The foundation of these ecosystems are reef-building scleractinian corals, whose calcareous skeletons construct the reef's physical structure (Hughes et al., 2017a; Moberg and Folke, 1999). Coral reefs are under threat of intensifying anthropogenic-induced stressors, particularly from global warming and elevated sea temperatures (Bozec et al., 2025; Hughes et al., 2020, 2017b; Ortiz et al., 2021; Otto, 2018; Virgen-Urcelay and Donner, 2023). Under such stressful conditions, corals can lose their symbiotic algae in a reversible process known as coral bleaching (Helgoe et al., 2024; Hoegh-Guldberg et al., 2007). As corals rely on their symbionts for metabolic inputs, persistent bleaching can result in widespread coral deaths (Sully et al., 2022). An estimated 14% of the world's coral cover has already been lost between 2009 and 2018 (Souter et al., 2021), and with bleaching-induced coral mortality on the rise (Bozec et al., 2025; Hughes et al., 2020, 2017b; Virgen-Urcelay and Donner, 2023) there is concern for the impact of climate change on coral reef structures, biodiversity, functioning and productivity globally (Graham et al., 2015; Hughes et al., 2019; Morais et al., 2022; Sully et al., 2022).

Despite increased frequency and intensity of mass bleaching events, corals appear to be adapting to repeated exposure of elevated temperatures (e.g., Bozec et al., 2025; Drury and Lirman, 2021; Louis et al., 2016; Palumbi et al., 2014; Schoepf et al., 2015). For example, increased thermal tolerance of coral communities has been observed around Palau in the Pacific Ocean in recent years following multiple acute bleaching events across the last few decades (Bruno et al., 2001; Lachs et al., 2023). While these trends could be attributed to acclimatisation, shifts in community structure or changes in the holobiont associations (Gouezo et al., 2019), contemporary within-population variation in coral heat tolerance indicates the possibility of an underlying genetic adaptation to elevated temperatures (Lachs et al., 2023; Mumby and Van Woesik, 2014). Indeed, studies using a variety of experimental methods (summarised in Selmoni et al., 2024) found that within-species thermal variation is heritable, with evidence arising from the Pacific Ocean (e.g., Bay and Palumbi, 2014; Selmoni et al., 2021, 2020a), the Great Barrier Reef of eastern Australia (e.g., Cooke et al., 2020; Dixon et al., 2015; Elder et al., 2022; Fuller et al., 2020; Jin et al., 2016; Lundgren et al., 2013; Quigley et al., 2020), the East Indian Ocean along the west Australian coast (e.g., Thomas et al., 2022, 2017), the Persian Gulf in the Middle East (e.g., Howells et al., 2021, 2016; Kirk et al., 2018; Smith et al., 2022), and the Caribbean Sea (e.g., Drury and Lirman, 2021; Dziedzic et al., 2019). As the heritability of thermal variation implies the existence of alleles that can promote tolerance to anticipated increased thermal regimes, identifying candidate genes and populations adapted to thermal stresses can provide valuable information for improving spatial mapping of reef vulnerability to inform reef restoration efforts (Selmoni et al., 2024).

Seascape genomics provides a promising framework for investigating adaptation to environmental stressors in *in-situ* populations located across diverse geographic and environmental ranges (Riginos et al., 2016; Selmoni et al., 2021, 2020a). Within this framework,

neutral population structuring and connectivity across large spatial extents can provide key insights for understanding how sea currents might affect the spread of adaptive alleles within and between coral populations (De Mita et al., 2013; Lotterhos and Whitlock, 2015; Matz et al., 2020; Selkoe et al., 2016; Selmoni et al., 2020a; Weersing and Toonen, 2009). Seascape genomics also provides a framework for correlating whole genome variation with environmental factors using genotype–environment associations (GEA). In this way, genes putatively involved in adaptation are identified while simultaneously providing insights into the environmental conditions that might be driving genetic differences (Rellstab et al., 2015). Significant associations from GEA correlations suggest candidate loci under selection, which, if reference genomes are available, can be used to highlight markers near or within a gene of interest to infer molecular functions under selection (Storfer et al., 2018). This is important, as long-term coral cover is expected to benefit from genetic influxes of thermally-adapted coral recruits originating from reefs experiencing temperatures 0.5˚C higher than the local average (Matz et al., 2020). To assist the long-term adaptive capacities of coral populations, it is imperative to understand connectivity between reefs and the genes involved in adaptation.

While strides are being made to understand coral thermal adaptations and thermal heritability globally, research gaps remain. First, research is predominantly concentrated around reef systems in the Indo-Pacific region, notably the Great Barrier Reef in Australia (summarised in Selmoni et al., 2024). For instance, early GEA methods successfully detected candidate genes under thermal selection in the Great Barrier Reef (Lundgren et al., 2013). However, large stretches of coral reef regions remain understudied despite coral bleaching responses varying within and among oceans, attributable to differences in regional thermal regimes, evolutionary histories, and past disturbances (Shlesinger and van Woesik, 2023). Notably, coral reefs in the West Indian Ocean (WIO) have been largely overlooked (Carr et al., 2025), despite hosting

approximately 5% of global coral reefs affected by recurrent short- and long-term bleaching events (Shlesinger and van Woesik, 2023; van Woesik and Kratochwill, 2022). With most WIO ecosystems labelled as vulnerable (e.g., Seychelles) to critically endangered (e.g., Mauritius Islands) due to human activities and global warming (Obura et al., 2022), more research is necessary in this region for informed biodiversity management. Second, research typically focuses either on contiguous reef systems or at local isolated reefs (Selmoni et al., 2024). Though marine environments are highly connected in general, where local stressors can have regional-level effects on community structures (Green et al., 1987), it remains unclear of how breaks in connectivity (>100 km of open sea) affect the spread of adaptive alleles between reefs of a network. Last, research into coral thermal adaptation is typically conducted on a single study species at a time (Selmoni et al., 2024; but see Selmoni et al., 2021). Diversity of morphologies and habitat preferences results in differential responses of corals to selection pressures and stressful events (Guest et al., 2012; Johnston et al., 2021; Yuen et al., 2023). For example, corals with branched morphologies are generally more sensitive to heat stress than those with massive morphologies (Loya et al., 2001). As evolutionary trajectories are species-specific, it seems that patterns of genomic diversity observed in one species cannot necessarily be extrapolated to others, yet conservation strategies must consider the needs of multiple species simultaneously (Voolstra et al., 2023).

Despite a growing body of research investigating coral connectivity between islands of the WIO (e.g., Carr et al., 2025; Gélin et al., 2018; Kusumoto et al., 2020; Oury et al., 2024; Vogt-Vincent et al., 2024), studies have yet to incorporate genetic data for investigating region-wide connectivity between Seychelles and the Mascarene Islands, with little investigation into the adaptive potentials of corals across the WIO region. Here, we aim to address these research gaps to better understand coral adaptive potential across large, non-contiguous reef networks. Specifically, we

investigate (i) the genetic connectivity of two keystone coral species with contrasting reproductive strategies across the WIO, and (ii) their molecular adaptations to thermal conditions. To this end, we applied a seascape genomics framework to detect coral reefs that putatively host thermal stress-adapted coral genotypes, to ultimately provide information that will support local stakeholders in developing regional biodiversity management plans in the WIO (Donovan et al., 2021; Goetze et al., 2021; Pittman et al., 2021; Stefanoudis et al., 2023).

2. Materials and Methods

We focus on two common WIO reef-building coral species, *Acropora muricata* and *Pocillopora damicornis*, sampled at reefs around the Seychelles in the northern WIO and Mauritius and Rodrigues of the Mascarene Islands group in the southern WIO (**Fig. 1a**). We first characterised the seascape conditions around each island using open-access satellite and geomorphic data, from which 15 reefs with contrasting environmental conditions were selected for coral sampling and genotyping. Our framework follows a seascape genomics approach (Selmoni et al., 2020a) to (i) map the connectivity of populations across the WIO region and (ii) identify putatively adaptive coral genotypes using genotype–environment association (GEA) analyses (**Suppl. Fig. 1**). By coupling these analyses, we then infer the spatial distribution of WIO reefs that potentially carry genotypes underpinning local adaptation to thermal stress for informed reef management planning. All analyses were performed in the R environment (R Core Team, 2024).

2.1 Study species

We selected *A. muricata* and *P. damicornis* for the present study as two common reef-building corals of the WIO that represent keystone species with high ecological relevance (Bridge et al., 2023; Cunning et al., 2018). Both species show evidence of population recovery after severe bleaching events (Bruno et al., 2001; Lachs et al., 2023), which could be attributed to thermal

173 tolerance (Ainsworth et al., 2016; Carr et al., 2025; Gouezo et al., 2019; Humanes et al., 2022),
174 such that they are interesting subjects for investigating adaptation to thermal stressors.
175 Furthermore, these species have distinct life history strategies that warrant independent
176 investigations of thermal tolerance and connectivity. *A. muricata* is a predominately broadcast
177 spawning coral, releasing gametes into the water column in synchronised events at the
178 beginning of the Austral summer (October to December) when sea temperatures increase
179 (Wijayanti et al., 2019). *P. damicornis* has mixed reproduction, with sexual reproduction via
180 year-round broadcast spawning (Gélin et al., 2018, 2017; Schmidt-Roach et al., 2012; Smith et al.,
181 2019; Ward, 1992).

182 **2.2 Sampling strategy**

183 Fifteen reefs were selected for sampling across three regions of the WIO: six sites around
184 Mauritius, six sites around the Seychelles (three each at Mahé and Praslin) and three sites
185 around Rodrigues (**Fig. 1a; Suppl. Table 1**). Reefs were selected following the methods of
186 Selmoni et al. (2020b) to maximise environmental contrast for improved power in seascape
187 genomic analyses, while simultaneously considering logistical constraints in collaboration with
188 local stakeholders, including site accessibility and weather conditions during sampling. Full
189 details are provided in the Supplementary Material (**Suppl. Methods: Selection of sample**
190 **sites**).

191 The field sampling campaign took place with the assistance of scientists and technical staff of the
192 Mauritius Oceanography Institute (MOI) in January and February 2022 for Mauritius and
193 Seychelles, and in May 2022 for Rodrigues. This sampling campaign was performed within the
194 framework of the Coral Reef Restoration Project of the United Nations Development
195 Programme Mauritius (PIMS 5736, sampling permit in Rodrigues SPA 30) and the Government
196 of Seychelles (sampling permit A0157). Colonies identified as *A. muricata* and *P. damicornis* were

sampled for genotyping within a radius of 250m from the coordinates of the sample site at depths between 2-10m, with up to 30 colonies sampled per site per species. Each sample consisted of a 2cm branch collected with pliers and bagged underwater, before being transferred to 80% ethanol and stored at -20˚C. A total of 345 *A. muricata* and 403 *P. damicornis* colonies were sampled for DNA extraction and single nucleotide polymorphism (SNP) genotyping (**Suppl. Table 1**).

2.3 Environmental characterisation

The seascapes at the 15 study reefs were characterised using 17 environmental and geomorphic variables that might be exerting selection pressures on corals. These variables were accessed from two publicly available online archives. Environmental variables pertaining to climatic conditions and proximity to anthropogenic activities covering the whole study extent were extracted from the Reef Environment Centralized Information System (RECIFS; Selmoni et al., 2023). These variables were accessed at 5 km^2 spatial resolutions and described as month-by-month environmental variation covering a temporal range of a minimum of 20 years up to December 2021 (i.e., when sampling took place; full details on variables are summarised in **Suppl. Table S2**). Temporal mean and standard deviations were then calculated for degree heating week (DHW; Skirving et al., 2020), sea surface temperature (SST; Skirving et al., 2020), chlorophyll (CHL) and suspended particulate matter (SPM), where CHL and SPM were obtained from the 'OCEANCOLOUR_GLO_BGC_L4_MY_009_104' dataset (accessed on 03-04-2014; E.U. Copernicus Marine Service Information (CMEMS), 2024). In addition to RECIFS environmental variables, we retrieved a geomorphic characterisation of the WIO reefs from the Allen Coral Atlas (ACA; Allen Coral Atlas, 2022). Available at 10m resolution, this variable was processed to calculate the proportion of reef slope, reef flat, back reef and reef plateau at each sampling site (250m radius around the sample site coordinates). A Spearman's pairwise non-parametric rank

221 correlation threshold of ρ<|0.8| was applied to retain uncorrelated variables for downstream
222 analyses (**Table 1**), where a principal component analysis (PCA) on scaled and centred
223 environmental variable values was used to characterise the study sites (**Fig. 1b**).

224 **2.4 DNA extraction and SNP genotyping**

225 DNA extraction and SNP genotyping followed methods of Selmoni et al. (2021). Briefly, DNA was
226 extracted using a DNeasy Blood and Tissue 96 kit (Qiagen) following the manufacturer's
227 instructions. DNA samples were sent to Diversity Arrays Technology (Canberra, Australia) for
228 quality check screening and genotype-by-sequencing using the DArT-sequencing method
229 (DArT-seq), using restriction enzymes *Pst*I and *Hpa*II (Gawroński et al., 2016; Kilian et al., 2012;
230 Selmoni et al., 2021). Sequencing read processing was performed by Diversity Arrays
231 Technology using proprietary DArT analytical pipelines (Sansaloni et al., 2011). To minimise
232 technical bias and potential batch effects, targeted *A. muricata* and *P. damicornis* samples were
233 kept separated and randomly distributed across the respective batches (e.g., 96-well plates,
234 sequencing lanes) throughout the workflow (DNA purification, library preparation and
235 sequencing). Raw sequence data have been deposited in the NCBI BioProject database under
236 accession number PRJNA1277000.

237 **2.5 SNP filtering**

238 The raw DArT-seq loci were aligned to each species' reference genomes using BLAST to retain
239 only the SNPs associated with the coral hosts (filtering thresholds: >70% percentage identity,
240 >80% overlap identity, and >50 bitscore). The reference genome for *A. muricata* was the
241 chromosome-level assembly of *Acropora millepora* (v2.1; GCF_013753865.1; Fuller et al., 2020),
242 and the reference genome for *P. damicornis* was the scaffold-level assembly of *P. damicornis* (v1;
243 GCF_003704095.1; Cunning et al., 2018).

244 SNP filtering was performed for each species separately. First, we filtered out individuals
245 sharing highly similar genotypes (Pearson pairwise correlations >0.95), retaining one individual
246 in cases where genetic similarity was found. We then removed SNPs and individuals with high
247 missing rates (>80%) before applying a filter to exclude rare alleles (minor allele frequency; MAF
248 <5%). As both species potentially include cryptic species (Gélin et al., 2018, 2017; Grupstra et
249 al., 2024; Johnston et al., 2017; Oury et al., 2024; Riginos et al., 2024), we used a principal
250 coordinate analysis (PCoA) of the genotype matrix to cluster individuals based on genomic
251 distance, before removing clusters with an F_{ST} difference >0.3 with the other clusters. These
252 individuals will hereafter be referred to as 'cryptic' individuals. We genetically confirmed the
253 species identity of retained *Pocillopora* samples as *P. damicornis* using DArT sequences within
254 the ITS-2 and 18S ribosomal DNA regions (**Suppl. Table S3**). We repeated the missingness and
255 MAF filtering steps on the retained individuals. Last, we assessed linkage disequilibrium (LD)
256 amongst SNPs using functions from the *dartR* R package (Mijangos et al., 2022) to create an LD
257 map of the genome, with a maximum pairwise limit of 15 kbp (the distance of estimated LD
258 decay to r^2<0.05, based on whole genome sequence data of *A. millipora*; Fuller et al., 2020)
259 before pruning SNPs with an LD >0.2. As we found minimal effect of LD pruning on population
260 structure (assessed using a PCoA), nor evidence of SNPs clumping in a PCA (assessed using
261 *PCAdapt*; Luu et al., 2017; Privé et al., 2020), we did not prune for LD and retained all loci for
262 downstream analyses.

263 **2.6 Neutral genetic structure**

264 We assessed the neutral genetic structure of each species using two complementary methods: i)
265 Principal Coordinate Analysis (PCoA) and ii) Sparse Nonnegative Matrix Factorization (sNMF).

266 We first produced a neutral genomic dataset, where we identified and removed outlier loci using
267 a genome scan of the filtered genotype matrix via the *pcadapt* R package (v4.3.5; Luu et al.,

2017; Privé et al., 2020). In short, loci were attributed p-values based on their Mahalanobis distances along the retained axes of a PCA of the genotype matrix (2 PCs for *A. muricata* and 3 PCs for *P. damicornis*). We calculated the false discovery rate (FDR; Storey and Tibshirani, 2003) to correct p-values for multiple testing using the *qvalue* R package (2.36.0; Storey et al 2024), with a q-value <0.05 threshold to identify and remove outlier loci for the neutral genotype matrix.

We assessed contemporary population structure using a Gower PCoA clustering mixture model through the *dartR* R package (v2.9.7; Gruber et al., 2018; Mijangos et al., 2022) based on a distance matrix from allele frequency differences amongst individuals. We retained 2 PCo axes for *A. muricata* and 3 PCo axes for *P. damicornis* before allocating individuals to population groups using a hierarchical cluster analysis. We assessed ancestral population structure using sNMF algorithms with the *LEA* R package (v3.16.0; Frichot and François, 2015). Using a cross-entropy validation for K=1–10 over five repetitions with an alpha=100, we identified the number of ancestral populations to retain, using the K values resulting in the lowest average cross entropy to compute the sNMF. Membership assignment of each individual to the K ancestral populations was represented as proportions in a barplot. We calculated genetic structure between the sample sites using *F*-statistics (Wright, 1969, 1978) through the *dartR* R package (Gruber et al., 2018; Mijangos et al., 2022), obtaining observed (H_O) and expected (H_E) heterozygosity levels to calculate the inbreeding coefficient (F_{IS}), alongside pairwise F_{ST} between sample sites.

2.7 Connectivity analysis

We ran a connectivity analysis to investigate how physical distances between reefs correspond to genetic separation between colonies, calculated using the pairwise F_{ST} index (Section 2.6). Physical distance between reefs were derived from sea current data, following methods of

Selmoni et al. (2020a). Briefly, we retrieved maps describing monthly average direction and strength of surface sea currents throughout the WIO. These maps are available at a spatial resolution of 0.083° across 30 years as satellite-derived reconstructions of sea currents (from the 'GLOBAL_REANALYSIS_PHY_001_030_104' dataset, accessed on 03-04-2014; E.U. Copernicus Marine Service Information (CMEMS), 2024), which are publicly available via RECIFS (Selmoni et al., 2023). For each pixel, we calculated the cumulative speed towards each of the eight neighbouring pixels and divided this by the total speed to obtain a probability of transition in each direction (the conductance). We then calculated the dispersal costs as the inverse of the square conductance to obtain transition matrices using the *gdistance* R package (v1.6.4, van Etten, 2017). Finally, we calculated the shortest sea distance (least-cost path) between pairs of sites in both directions from the transition matrix to obtain an asymmetrical square matrix of shortest sea distance.

To determine the best predictor of genetic distance between reefs, we built a set of linear connectivity models to estimate F_{ST} as a function of the shortest in-water sea distance between sample sites. We built one model per month, and one based on annual average sea currents (13 models total). We also investigated the predictive performance of Euclidean geographic distances as an independent comparison model calculated from cartesian coordinates of sampled reefs. Models were built using a log-log relationship between F_{ST} and physical distance (i.e., sea distance and geographic distance). Their predictive powers were assessed using a leave-one-reef-out jackknife resampling approach, where model performance was assessed using coefficients of determination (R^2). Predictions of genetic connectivity among sites were obtained by translating the unit of sea distance into a unit of genetic separation (F_{ST}) through a linear model, using the connectivity predictor that best explained F_{ST} values.

2.8 Genotype–environment associations (GEA)

316 We performed GEAs using multivariate redundancy analyses (RDA) at the population-level
317 following methods of Capblancq and Forester (2021). The genotype response matrices were
318 coded as allele frequencies, where missing data was imputed from the median of the locus-
319 specific allele frequency across all populations (missingness per site for *A. muricata*: S04 with
320 0.05%, S05 with 0.04%, S07 with 0.14%; and for *P. damicornis*: S04 with 0.01%, S09 with
321 0.06%). The environmental variables used in the explanatory matrix were selected from the 10
322 uncorrelated variables (**Table 1**) using an autonomised forward and backward stepwise model
323 selection procedure with 10,000 permutations through the *ordistep* function of the *vegan*
324 package. We first ran a preliminary RDA to identify environmental variables explaining neutral
325 genomic variation. This procedure selected the standard deviation of monthly sea surface
326 temperature (sSST) and average monthly maximal DHW (mDHW) as the variables that best
327 explained neutral genetic variation independently for both species. To detect putative genomic
328 regions under selection, we performed a multivariate GEA using a partial RDA on the entire
329 genotype matrix and included reef-level population structure as a conditional variable to control
330 for neutral genetic variation. Controlling for neutral genetic variation was done to reduce false-
331 positive detections at the expense of losing power to detect true outlier loci along neutral
332 gradients (Excoffier et al., 2009; Lotterhos, 2023). The values representing population structure
333 were obtained from the axes of a PCA of centred and scaled neutral allele frequencies using the
334 *rda* function of the *vegan* R package, retaining the first *K* PCs that explained more than the mean
335 explained variance.

336 Outlier loci were identified from RDA loadings (Capblancq et al., 2018). After retaining all
337 constrained RDA axes (K=2 for both species), we evaluated the significance of each SNP based
338 on the extremeness of its Mahalanobis distance value compared to the distribution of the other
339 SNPs in the RDA space. The Mahalanobis distances were computed using the *dist_ogk* function

340 of the *bigutilsr* R package (v.0.3.4; Privé, 2021), corrected for genomic inflation factor (François
341 et al., 2016) and distributed along a chi-squared distribution with *K* degrees of freedom to assign
342 a p-value to each SNP (Luu et al., 2017). We applied an FDR threshold of *q*-value<0.05 to identify
343 outlier loci.

344 **2.9 Gene Ontology (GO) enrichment analysis**

345 Gene Ontology (GO) enrichment analyses were used to assess the putative molecular function(s)
346 of significant outlier SNPs (i.e., those with *q*-value <0.05) detected with the two heat-related
347 variables (sSST and mDHW) for both species, following Selmoni et al. (2021). To facilitate
348 comparability of annotation between species, we re-annotated genes in both reference
349 genomes. For this, we retrieved transcript sequences of each gene, then ran a similarity search
350 (blastx) against a manually curated database of protein sequences and annotations
351 (Uniprot/swissprot, metazoan entries as accessed on November 2022; Boeckmann et al., 2003).
352 Protein annotations were assigned to the coral genes when the E-score of the similarity search
353 was $<10^{-6}$. We then identified genes located within ±10 kbp of significant SNPs from the GEA
354 analysis (hereafter "significant genes"; Selmoni et al., 2021). We evaluated gene-set enrichment
355 of significant genes using the *SetRank* R package (version 1.0; Simillion et al., 2017), where
356 genes are ranked based on ascending *q*-values from the GEA from which overrepresented GO
357 terms associated with significant genes are identified. GO terms were deemed significant when
358 they had *SetRank p*-values<0.01 and adjusted *p*-values<0.05 (i.e., corrected for multiple testing
359 and overlap between gene-set categories).

360 **2.10 Adaptive Potential Index (API)**

361 The potential of corals to adapt to temperature increases depends on (i) the thermal history at
362 the reef (and therefore local adaptation of populations) and (ii) the arrival of propagules from

363 neighbouring heat-adapted reefs (Matz et al., 2020; Selmoni et al., 2020a). Building on previous
364 adaptation indices, including the Population Adaptive Index (Bonin et al., 2007) and the
365 Landscape Adaptive Index (Zhang et al., 2019), we calculated a spatially explicit 'Adaptive
366 Potential Index' (API) by combining results from the GEA (Section 2.7) and the connectivity
367 analyses (Section 2.9). To summarise potential for local adaptation, first we calculated an
368 'Adaptive Score' to link putatively adapted alleles with the thermal history of reefs across the
369 WIO (Capblancq et al., 2020). For this, we ran an RDA associating the outlier loci from the GEA
370 (Section 2.7) with the thermal explanatory variables (i.e., sSST and mDWH). The environmental
371 scores from these RDA axes were extracted and normalised to a scale of 0-1 to obtain an
372 Adaptive Score (Steane et al., 2014). The Adaptive Score was then projected across the WIO
373 reefs using thermal history data for each reef of the region. Second, we calculated the 'Inbound
374 Connectivity Index' (ICI) and 'Outbound Connectivity Index' (OCI) for each reef, which represent
375 the total neighbouring reef areas located downstream or upstream of a target cell, respectively,
376 limited to a sea distance equivalent to the species' $F_{ST} \leq 0.1$ (Section 2.9). Finally, we calculated
377 the Adaptive Potential Index for each reef cell as the total area of inbound connected reefs with
378 an Adaptive Score >0.8.

379 **3. Results**

380 **3.1 Site characteristics and genomic filtering**

381 Across the 15 reefs selected for coral sampling, six sites were sampled in the Seychelles (three
382 each at Mahé and Praslin), six in Mauritius and three in Rodrigues (**Fig. 1a**). These reefs
383 represent contrasting environmental conditions (**Fig. 1b**), as characterised by 10 uncorrelated
384 environmental variables (**Table 1; Suppl. Fig. S2**). The northern-most sampled reefs were those
385 from the Seychelles (represented in red), comprising predominantly of back reefs located near
386 deep water with less thermal stress (i.e., low sSST and low mDHW), generally further away from

387 human activity (i.e.., cropland, human population and boat activity). Most Mauritian reefs
388 (represented in blue) are characterised by reef flats near land and human activity (i.e., cropland
389 and boats) that experience more variable thermal conditions. The exception is the more isolated
390 northern-most Mauritian site on Ile Plate (S12 in dark blue), which is associated with deeper
391 waters and more stable temperatures. Finally, the three reefs at Rodrigues (represented in
392 green) are isolated reef flats located near deeper water that experience hotter (higher mDHW)
393 and more variable SST conditions (sSST).

394 Between 8–29 individuals per species were sampled for genotyping at each site (**Fig. 1a;**
395 **Suppl. Table S1**). The DArT-seq analytical pipeline resulted in 73,253 bi-allelic SNPs genotyped
396 for 345 *A. muricata* individuals and 65,708 SNPs for 403 *P. damicornis* individuals (values of
397 SNPs and individuals retained at each step are summarised in **Suppl. Table S4**). We removed
398 48 *A. muricata* and 261 *P. damicornis* individuals identified as clones, followed by 49 *A.*
399 *muricata* and 8 *P. damicornis* individuals with too much missing data and low MAF, and a
400 further 43 *A. muricata* and 14 *P. damicornis* individuals identified as cryptic individuals (i.e.,
401 F_{ST}>0.3 between PCoA clusters). We used pairwise F_{ST} and PCoA biplots to confirm that these
402 cryptic individuals were removed from the dataset (**Suppl. Fig. S3**). After filtering for rare
403 variants, missing values, clones and cryptic individuals, our final genotype matrix comprised of
404 205 *A. muricata* individuals with 5,757 SNPs and 120 *P. damicornis* individuals with 12,953
405 SNPs. This resulted in 4–7 *A. muricata* individuals retained from 14 sites (no individuals were
406 left at Curieuse Reef (S06) in Seychelles), and 3–14 *P. damicornis* individuals retained across all
407 15 sites (**Suppl. Table S1**).

408 **3.2 Neutral genetic structure**

409 Outlier loci were identified and removed using a genome scan via the *pcadapt* R package to
410 produce a neutral genotype matrix for assessing population structure across the WIO. For the

411 genome scan, we retained *K*=2 PCs for *A. muricata* and *K*=3 PCs for *P. damicornis*, identifying 74
412 and 138 outlier SNPs (q-value<0.05), respectively. The final neutral genotype matrices
413 comprised of 5,683 SNPs for *A. muricata* and 12,815 SNPs for *P. damicornis* (**Suppl. Table S4**).

414 We found strong population structuring for *A. muricata*, where PCoA and sNMF models indicate
415 the presence of three genetic clusters strongly associated with geographic distributions (**Fig.**
416 **2a**). Furthermore, we find evidence of high gene flow between reefs within regions contrasted
417 with stronger genetic differentiation between regions. Indeed, the first two PCoA axes (capturing
418 almost 20% of neutral genetic variation) assigned individuals into groups closely reflecting
419 sampled regions **(Fig. 2ai)**, with sNMF models confirming that individuals are genetically similar
420 within regions with low gene flow between regions (**Fig. 2aii-iii)**. These patterns are
421 statistically supported by AMOVAs, where genomic variance is significantly higher between
422 regions than expected by chance (p<0.01; **Suppl. Fig. S4a**). In contrast, variance between sites
423 within regions and variance between subregions were not significant. Low pairwise F_{ST} values
424 (i.e., F_{ST}≤0.01) further substantiates substantial gene flow with limited genetic differentiation
425 between reefs of the same region (**Table 2**). In contrast, pairwise F_{ST} values between certain
426 regions exceeded 0.20, signalling restricted gene flow and increased genetic divergence between
427 more distant regions (**Table 2**); larger F_{ST} values (i.e., F_{ST}≥0.20) were between reefs at the
428 Seychelles with Rodrigues, as well as between site S04 on the western side of Mahé (SEY) with
429 reefs around the main islands of Mauritius. Last, high inbreeding coefficients (F_{IS}>0.20) were
430 observed between reefs of the Seychelles, Rodrigues, and the northern and southern reefs of
431 Mauritius (**Suppl. Table S5a**), further pointing towards restricted gene flow between reefs of
432 different regions.

433 Four genetic clusters were identified for *P. damicornis* across the three geographic regions using
434 PCoA (first two axes capturing 23% of neutral genetic variance) and sNMF. The genetic clusters

435 roughly matched geographic location, with evidence of some gene flow between geographic
436 regions (**Fig. 2b**). AMOVA analyses indicate that genomic variance is significantly higher
437 between sites (p<0.01) and between regions (p=0.03) than expected by chance, while variance
438 between subregions were not significant (**Suppl. Fig. S4b**). There appears to be strong genetic
439 similarities between individuals in the northern and southern Mauritius reefs with individuals in
440 Rodrigues, as well as with some individuals in the northern Seychelles (Praslin) reefs (yellow
441 clusters in **Fig. 2b**). Within regions, reefs had varying levels of genetic differentiation, with
442 pairwise F_{ST} values between -0.01 and 0.16. Most individual genetic similarity was between the
443 Rodrigues reefs, while the largest differences were between the Mauritius island reefs (**Table 2**).
444 Between regions, the largest differences were between the eastern and western reefs of
445 Mauritius with the Seychelles (F_{ST}≥0.15), while the most similar regions are between those of
446 the Mascarene Islands (i.e., Mauritius and Rodrigues; F_{ST}<0.15). Finally, most sites had evidence
447 of panmixia, though higher than expected homozygosity (F_{IS}≥0.20) was observed at the
448 eastern-most reef of the Seychelles (S07), as well as at the northern (S12) and southern (S01)
449 Mauritius reefs (**Suppl. Table S5b**).

450 **3.3 Connectivity Analysis**

451 Genetic connectivity between *A. muricata* populations was well explained by sea currents and
452 geographic distance, with a median R^2 of 0.80 (range of median R^2 0.67–0.87) across all
453 predictors following a leave-one-reef-out jackknife analysis (**Fig. 3ai**). The best predictor of F_{ST}
454 was mean sea current in December with a median R^2 of 0.87 (IQR 0.86–0.87; **Fig. 3ai**). Genetic
455 connectivity between *P. damicornis* populations was also well explained by sea currents, albeit to
456 a lesser degree than for *A. muricata*. Monthly sea currents all had similar strengths to predict
457 patterns of genetic connectivity of *P. damicornis* across the WIO, with associations producing a
458 median R^2 of 0.36 (range of median R^2 0.26–0.38; **Fig. 3bi**). Geographic distance again

459 explained less genetic connectivity than sea currents, with a median R^2 of 0.26 (IQR 0.25–0.40).
460 We therefore chose to model the genetic connectivity of *P. damicornis* using the average annual
461 sea current, which explained 36% of the F_{ST} variation (median R^2 of 0.36; IQR 0.35–0.39; **Fig.**
462 **3bi**).

463 The species-specific $\log_{10}$–$\log_{10}$ relationships between F_{ST} and optimised sea distance (based on
464 December currents for *A. muricata* and annual currents for *P. damicornis*) indicate a stronger
465 relationship by approximately 3.5 times for *A. muricata* than for *P. damicornis*, with respective
466 regression coefficients of 0.885 (**Fig. 3aii**) and 0.238 (**Fig. 3bii**). These results reiterate patterns
467 of neutral gene flow observed between regions for both species (see Section 3.2), where *A.*
468 *muricata* individuals were more genetically similar between closer reefs and more genetically
469 dissimilar with further reefs, while the weaker relationship for *P. damicornis* highlights that
470 physical distance does not necessarily correspond with genetic similarity amongst individuals.

471 **3.4 Genotype–Environment Associations to identify loci under selection**

472 The two thermal stress variables, sSST and mDHW, best explained reef-level neutral genetic
473 variation for both *A. muricata* and *P. damicornis*, as determined using an automated forward
474 and backward variable selection method. As a preliminary partial RDA revealed confounding
475 effects of neutral genetic structure and thermal stress, we performed GEA analyses while
476 accounting for neutral structure using 3 PCs for *A. muricata* (explaining 68.4% variance) and 4
477 PCs for *P. damicornis* (explaining 64.2% variance) to reduce false positive outlier loci.

478 For *A. muricata*, the first and second pRDA axes respectively explained 21.0% and 5.8% of
479 genetic variation (**Fig. 4ai**). Both axes were negatively associated with sSST and mDHW, with
480 the second axis showing a stronger association with mDHW. A total of 380 outlier loci were
481 identified (q-value<0.05) throughout the genome (**Fig. 3aii**). SetRank analyses revealed that

482 significant genes (i.e., those within ±10 kbp of significant SNPs) were associated with seven
483 enriched GO terms (molecular functions) and encode five proteins: glycine receptor subunit
484 alpha-3 (GO:0022852), putative beta-hexosaminidase (GO:0030247, GO:0004563), protein
485 SGT1 homolog (GO:0051087), Sacsin (GO:0070628, GO:0030544) and Glutathione S-
486 transferase omega-1 (GO: 0045174) (**Fig. 4aiii**). Interestingly, six genes significantly
487 associated with temperature were annotated as Sacsin (DNAJC29) and SGT1 homolog proteins,
488 which have the molecular function "chaperone binding activity" (of these, five genes were also
489 associated with "Hsp70 protein binding activity"). The other significant genes included those
490 associated with glycine-gated chloride ion channel activity (two genes), polysaccharide binding
491 activity (specifically with beta-N-acetylhexosaminidase activity; four genes), and glutathione
492 dehydrogenase activity (two genes).

493 In *P. damicornis*, the first pRDA axis explained 17.8% of genetic variation and was negatively
494 associated with sSST, while the second partial RDA axis explained 16.9% of genetic variation
495 and was negatively associated with mDHW (**Fig. 4bi**). A total of 292 outlier loci were identified
496 (**Fig. 3bii).** SetRank enrichment analyses identified only carbon-sulfur lyase activity
497 (GO:0016846) as an enriched molecular function by four significant genes that are associated
498 with centromere protein V (**Fig. 4biii**).

499 **3.5 Adaptive Potential Index (API) across the West Indian Ocean**

500 We combined network-level connectivity models with spatial distributions of putatively heat-
501 adapted genotypes to produce an Adaptive Potential Index (API) across the WIO for identifying
502 donor reefs with the potential to disperse thermal-adapted genotypes to neighbouring reefs
503 (**Table 3**). For a given pixel, the API represents the surface area (in km^2) of neighbouring reefs
504 that (1) have a thermal history linked to the presence of candidate adaptive loci (Adaptive Score

≥0.8) and (2) are within a sea distance indicative of inbound connectivity (i.e., a distance that corresponds to an F_{ST} ≤0.1 upstream of the target reef). For both species, Adaptive Scores (AS) and API were region-specific, with higher values in more southern reefs at Mauritius and Rodrigues and lower values at reefs near the equator at the Seychelles (**Fig. 3iii; Table 3; Supp Fig. S5**).

For *A. muricata* (**Fig. 3aiii; Table 3**), the reefs around Mauritius hosted moderately heat adapted corals (AS between 0.43–0.74), further receiving adapted propagules from an estimated 181–187 km^2 of other reefs. While *A. muricata* at the Rodrigues reefs had slightly reduced API values (136 km^2) due to fewer heat adapted propagules up-current, these corals had the highest Adaptive Scores (AS ≥0.80) of the studied reefs, supplying propagules to almost 700 km^2 of reefs downstream (OCI). In the northern WIO, *A. muricata* corals of the Seychelles had both lower thermal Adaptive Scores (AS <0.16) and the lowest API with heat adapted propagules coming from an estimated 41 km^2 of reefs (API), despite these reefs being connected to approximately 1550 km^2 of reefs upstream (ICI) and >935 km^2 downstream (OCI).

Similar AS estimates of coral adaptation to thermal stress and patterns of API were observed for *P. damicornis*, where connectivity measurements based on weaker F_{ST} relationships with sea currents resulted in lower values for IBI, OCI and API (**Fig. 3biii; Table 3**). The reefs at Mauritius and Rodrigues appear to host the most heat adapted corals (AS between 0.41–0.81), respectively receiving heat adapted propagules from an estimated 102 km^2 and 94 km^2 of reef (API) and providing adapted propagules to approximately 300 km^2 and 450 km^2 of reef (OCI). In the Seychelles, *P. damicornis* corals had very low adaptive scores (AS <0.17) and were expected to receive no adapted propagules (API of 0 km^2) from the 811–870 km^2 of inbound connected reefs.

4. Discussion

529 **4.1 Life-history traits and asymmetric ocean currents drive population structure across**
530 **the WIO**

531 Coupling genomic information with environmental data revealed the importance of coral life-
532 history strategies and asymmetrical ocean currents in driving spatial patterns of population
533 structure across the WIO. The population structure uncovered in this study corroborates
534 connectivity simulations and mapped genetic structuring of various other coral species across
535 the WIO (e.g., Gélin et al., 2018; Kusumoto et al., 2020; Oury et al., 2024; Vogt-Vincent et al.,
536 2024).

537 *A. muricata* showed strong patterns of local genetic mixing with minimal between-region gene
538 flow across the WIO, mirroring expectations for a synchronous broadcast spawning coral
539 species (Miller and Ayre, 2008). Indeed, high gene flow between reefs of a region within a
540 relatively short distance has been found for numerous Acroporidae around the world (e.g., Adam
541 et al., 2022; Fuller et al., 2020; Lukoschek et al., 2016; Nakajima et al., 2010; Selmoni et al.,
542 2021). Genetic mixing is promoted by synchronous release of gametes (Wijayanti et al., 2019),
543 while a free-swimming larval stage allows propagule dispersal to neighbouring reefs (Tabitha et
544 al., 2021). Some gene flow occurs between southern reefs of the Mascarene Islands (Mauritius
545 and Rodrigues) in a predominately westward direction along ocean currents (Vogt-Vincent et al.,
546 2024). However, corals in the Seychelles appear to be genetically isolated, where gene flow in the
547 Austral summer during *A. muricata* spawning is blocked by the strong oceanographic barrier of
548 the South Equatorial Countercurrent (at approximate latitude of 10° S; Phillips et al., 2021).

549 Similar, albeit more complex, population structuring was found for *P. damicornis* with three
550 region-specific genetic clusters and a fourth dispersed genetic cluster (yellow group in **Fig. 2b**).
551 The general pattern of gene flow between the Mascarene Islands reflects that observed for the *A.*
552 *muricata* populations and that of previous investigations into *P. damicornis* Type β dispersal

553 across the southern WIO (Gélin et al., 2018). The genetic dissimilarity observed for our *P.*
554 *damicornis* between the northern and southern regions can again be explained by strong ocean
555 currents (Phillips et al., 2021). The fourth genetic cluster poses an interesting complexity,
556 potentially attributed to contemporary gene flow, remnants of a common ancestral population,
557 and/or the inclusion of cryptic species or ecotypes in our analyses. Contemporary region-wide
558 gene flow might be facilitated by a well provisioned larval stage with up to 14 weeks viability
559 (Gélin et al., 2018, 2017; Richmond, 1987), where propagules can survive long distances,
560 travelling passively by ocean currents (Phillips et al., 2021), rafting (Nikula et al., 2013), or in
561 boat ballast water or hull fouling (Gollasch, 2008). Alternatively, this anomalous genetic cluster
562 could represent genetic remnants of a common ancestral population (Oury et al., 2024) that
563 expanded across the WIO following the penultimate glacial period (ca. 100,000 years ago) under
564 altered sea current conditions (Colleoni et al., 2016; Herbert et al., 2010). Evidence of ancestral
565 genetic make-up could be preserved by high rates of selfing and asexual reproduction of *P.*
566 *damicornis* (indeed, 65% of our samples were clones). Finally, the genetic cluster could simply
567 represent the inclusion of hybridised individuals, either between closely related cryptic species
568 occurring in sympatry (Carr et al., 2025; Combosch and Vollmer, 2015; Gélin et al., 2018; Oury et
569 al., 2024) or between colonies of genetically divergent and locally adapted ecotypes (e.g., shallow
570 lagoon ecotypes mating with outer reef slope ecotypes; Oury et al., 2024).

571 Regardless of the mechanism, population structure is rarely a simple function of reproductive
572 mode or larval type (Miller and Ayre, 2008; Prata et al., 2024; Severance and Karl, 2006). While
573 genetic exchange seems to occur across the southern WIO from Rodrigues towards the other
574 Mascarene Island reefs, and potentially beyond to Madagascar and the African east coast, the
575 South Equatorial Countercurrent barrier is undoubtedly inhibiting gene flow between southern
576 to northern WIO reefs near the equator (e.g., Seychelles). This can have important

consequences for adapted genotype exchange across the WIO, with impacts on management strategies to be implemented in different regions (Phillips et al., 2021; Vogt-Vincent et al., 2024). More wide-spread genetic sampling of corals is required to draw precise conclusions of population structure across the WIO region.

4.2 Sea currents as a proxy for genetic connectivity and dispersal

Using sea currents to determine asymmetric distance between reefs was a better predictor of population connectivity than Euclidean geographic distance for both coral species, supporting the growing body of literature calculating gene flow for marine organisms (e.g, Benestan et al., 2016; Cooke et al., 2016; Hernawan et al., 2023; Krueck et al., 2020; Prata et al., 2024; Snead et al., 2023; Villastrigo et al., 2023; White et al., 2010). For synchronous broadcast spawning corals, we might expect that genetic distance would be best predicted using sea currents from a particular time of the year. Indeed, connectivity of *A. muricata* was best predicted by sea currents in December, reflecting timing of known mass spawning for this species (Wijayanti et al., 2019). When no month's sea currents clearly explain genetic distance, such as for *P. damicornis*, it may be that the species has asynchronous spawning and potentially complex reproductive modes.

The correlation (r^2) and regression coefficients (m) of the connectivity models can also provide information about the pattern and strength of sea currents used to disperse the propagules across a reef network. A strong correlation coefficient seems to indicate more local recruitment of propagules, such as for *A. muricata* (r^2 =0.87), while weaker correlation coefficients indicate decoupling of gene flow from physical geographic distance, such as for *P. damicornis* (r^2 =0.37). The regression coefficient provides a rough estimate of length of larval stage, where the 3.5 times steeper regression coefficient of *A. muricata* vs *P. damicornis* (m =0.88 vs. m =0.24) mirrors the much shorter larval stage (3 weeks vs 14 weeks; Richmond, 1987; Tabitha et al., 2021). By using metrics derived from the connectivity model, hypotheses of life history

strategies can be obtained for non-model coral species to facilitate the development of appropriate management strategies.

4.3 Thermal stress drives signals of local adaptation

Historical thermal variation was found to correlate with non-neutral genetic diversity of two coral species across the WIO. Multivariate genotype–environment associations (GEAs) suggest local adaptation to thermal stress, with 380 and 292 outlier SNPs for *A. muricata* and *P. damicornis*, respectively, significantly associated with standard deviations in sea surface temperatures (sSST ; Skirving et al., 2020) and mean degree heating weeks (mDHW; Skirving et al., 2020). In both species, corals from Rodrigues exhibited the strongest signals of thermal adaptation, likely due to the higher and more fluctuating temperatures of its lagoon and reef flat environments. In contrast, corals from the Seychelles showed the weakest adaptive signals, as their backreef and reef slope habitats are influenced by cooler upwelling waters. These findings reflect recent evidence of mean SST as a strong predictor of global genetic diversity in *P. damicornis*, with highest nucleotide diversity at reefs experiencing higher temperatures (Carr et al., 2025).

Extreme and variable marine thermal conditions can trigger coral bleaching when SST fluctuations exceed seasonal averages (Hughes et al., 2017b; Liu et al., 2003), a pattern observed across the Indian Ocean (Shlesinger and van Woesik, 2023). Recurrent mass-bleaching events over decades exert strong selective pressures (Hughes et al., 2017b; Skirving et al., 2020), likely driving molecular signatures of thermal adaptation and tolerance in affected populations (Lachs et al., 2023). SST variation and mean DHW capture both the duration and intensity of thermal anomalies (Humanes et al., 2022; Liu et al., 2003; Skirving et al., 2020; van Hooidonk et al., 2016), which may explain the high number of outlier loci associated with heat stress detected here. While environmental data were extracted at 5 km resolutions, we acknowledge that reef

systems can exhibit substantial microhabitat variation at much finer spatial scales (e.g., <100m), potentially influencing highly localised patterns of coral adaptation (e.g., Bay and Palumbi, 2014; Bozec et al., 2025). To mitigate this effect, we standardised sampling depth between sites and used variables from the Allen Coral Atlas (at 10m resolution) to refine the ecological characterisation of each sample site. Nonetheless, the potential for undetected fine-scale environmental heterogeneity remains a limitation here.

4.4 Candidate molecular targets of heat stress

Genes near SNPs significantly associated with historical heat stress exposure (sSST and mDHW) had molecular functions that were previously observed in coral thermal responses. Interestingly, we found significant enrichment for heat shock proteins and molecular chaperones in *A. muricata*, driven by the presence of five significant genes encoding the Sacsin protein. Sacsin is a co-chaperone for the heat-shock protein Hsp70 (Ménade et al., 2018; Parfitt et al., 2009) and is significantly up-regulated when *Acropora* and *Pocillopora* species are exposed to high temperatures in lab conditions (Cunning et al., 2018; Cunning and Baker, 2014; Hemond et al., 2014; Mayfield et al., 2018). Sacsin has previously been identified as a key candidate protein involved in thermal responses of *A. millepora* in the Great Barrier Reef (Fuller et al., 2020), while another seascape genomic study on *A. millepora* in New Caledonia found significant enrichment of chaperone binding proteins associated with bleaching alert frequency (Selmoni et al., 2021).

Three other molecular functions were significantly enriched for *A. muricata* in association with thermal stress. The glutathione S-transferase omega-1 (EC 2.5.1.18) enzyme was detected with two significant genes associated with sSST and mDHW. This enzyme is upregulated in some coral species following long-term (60 day) heat stress exposure (Dias et al., 2019). This enzyme plays a key role in coral cellular antioxidant and immune defence responses (Morrow et al.,

649 2012), likely responding to reactive oxygen species induced by enhanced metabolic rates
650 (Burdon et al., 1990; Richier et al., 2006). We also found enrichment for the lysosomal enzyme
651 beta-hexosaminidase (EC 3.2.1.52) from four genes. This is an important factor involved in a
652 range of functions, including glycosylation of proteins, cellular signalling, protein folding, and
653 mycobacterium defence (Koo et al., 2008; Lundgren et al., 2013; Sproles et al., 2019). As
654 stressed corals have increased susceptibility to disease (Littman et al., 2010; Mydlarz et al.,
655 2010; Thurber et al., 2009), an adaptive increase in immune responses due to increased
656 temperatures might be expected (Lundgren et al., 2013). Last, the glycine receptor (subunit
657 alpha-3) protein associated with glycine-gated chloride ion channel activity was detected by
658 two genes, which is involved in synaptic signalling of the central nervous system of vertebrates
659 (Ceder et al., 2024) that might alter mobility and movement for feeding in heat-adapted corals.

660 Among heat-associated SNPs in *P. damicornis*, only one molecular function was significantly
661 enriched: carbon-sulphur lyase activity. To our knowledge, this function has not been previously
662 associated with heat stress and may represent a false signal. Given that previous studies on
663 *Pocillopora* spp. identified candidate genes involved in immunity, cellular homeostasis,
664 metabolism, and signalling responses to environmental stress (Lundgren et al., 2013; Mayfield et
665 al., 2018; Poquita-Du et al., 2024; Selmoni et al., 2021), we expected a greater number of
666 significant functional associations. The limited detection of enriched functions may be
667 attributed to the strong population structure observed, which we attempted to control for by
668 including neutral genetic structure in our RDA analysis. In this way, we targeted shared genomic
669 pathways involved in thermal stress responses amongst diverged individuals, where we cannot
670 rule out the retention cryptic or hybrid individuals in our dataset that inhabit different niches
671 and express different responses to stressors (Johnston et al., 2017). Alternatively, a lack of signal

672 may be attributed to the high proportion of unique, predominantly unannotated genes in *P.*
673 *damicornis*, which comprise up to a quarter of its genome (Cunning et al., 2018).

674 We stress caution in over-interpreting results of GEA and GO term analyses. These models
675 generate hypotheses to facilitate understandings of environmental influence on genotypes
676 (Lasky et al., 2023; Lotterhos, 2023; Selmoni et al., 2024). Candidate genes should therefore be
677 treated as preliminary results requiring experimental or in-field validations (reviewed in
678 Selmoni et al., 2024). Furthermore, numerous analytical factors can affect GEA results. Here, we
679 traded GEA power with reduced false positive rates when we corrected for population structure
680 (Forester et al., 2018; Lotterhos, 2023). GEAs also have reduced power to detect quantitative
681 trait nucleotides (Lotterhos, 2023); because polygenic variation is expected to drive coral
682 thermal adaptation (Rose et al., 2018), important genomic regions under selection are likely
683 missed. Additional methods, such as genome-wide association studies (GWAS) or quantitative
684 trait locus (QTL) mapping, could help strengthen conclusions drawn from seascape genomic
685 studies (Lasky et al., 2023; Lotterhos, 2023), as could the inclusion of other genomic variants
686 that are expected to play a major role in facilitating adaptation (e.g., structural variants; Mérot et
687 al., 2020; Pokrovac and Pezer, 2022; Wellenreuther et al., 2019). Nevertheless, our results
688 provide valuable hypotheses of genomic regions conserved across populations in response to
689 thermal pressures across a discontinuous reef system to guide future coral research and assist
690 regional coral reef management.

691 **4.5 Local-level reef management is recommended across the West Indian Ocean**

692 Coral reef ecosystems across the WIO are vulnerable to collapse under projected climatic
693 conditions (Obura et al., 2022). As local scale stressors can affect regional level community
694 structure (Green et al., 1987), we echo recommendations for coordinated local level
695 management across the WIO to maintain overall coral reef health (Obura et al., 2022;

Stefanoudis et al., 2023). We found that the large distances between reefs reduced the importance of regional gene flow for facilitating thermal adaptation. Indeed, the reef regions investigated represent two independent ecoregions (Obura, 2012; Spalding et al., 2007). Furthermore, coral propagule dispersal simulations across the WIO estimates that there are over 100 generational steps of separation (about 500 years) between the Mascarene Islands and the Seychelles (Vogt-Vincent et al., 2024). As congruent spatial pattens of the adaptive potential index (API) were observed for both species despite differences in life-history traits, demography and adaptation, we recommend similar management strategies for both species.

Understandings of source locations of thermally adapted corals and connectivity with other reefs in the region can help guide conservation planning (Bozec et al., 2025; Selmoni et al., 2024, 2020a). For instance, reefs hosting corals with higher adaptive potentials could be placed in a marine protected area (Abelson et al., 2016; De Clippele et al., 2023), while reefs with low adaptive potentials might require assisted gene flow from adapted reefs (Baums, 2008; Hagedorn et al., 2021; Van Oppen et al., 2015). The Mascarene Islands are important sources of heat adapted corals due to exposure to higher temperatures with large daily fluctuations across reef lagoons and flats. As the Mascarene Islands are located up-current of Madagascar and the east African coast along the South Equatorial Current (Phillips et al., 2021; Vogt-Vincent et al., 2024), these reefs may serve as important sources of thermal resilience for west WIO populations (Matz et al., 2020; Oury et al., 2024). In contrast, the Seychelles Archipelago appears to host fewer heat adapted corals, likely due to proximity with deep oceans and upwelling that bring cooler and more consistent water temperatures (Shlesinger and van Woesik, 2023). With their relative isolation, coral reefs of the Seychelles may require assisted gene flow, importing propagules from heat adapted reefs such as east African reefs that have already experienced recurrent mass bleaching (Elma et al., 2023).

Going forward, insights obtained from these seascape genomic analyses can be integrated into management frameworks that must be co-developed with local stakeholders (Stefanoudis et al., 2023). This is important to facilitate collaboration between local managers across the regional network to standardise research and management methods, share resources and undertake research that is directly relevant to making decisions for the overall health of the coral reef ecosystem in the WIO. Extrapolations of genetic-based adaptive indices to unsampled regions can be biased, particularly if predictor variables covary differently in training vs extrapolated reefs (Yates et al., 2018), or if genetic variation is not well distributed across the environmental landscape (Capblancq and Forester, 2021). Future work will need to include seascape genomic analyses across the larger WIO network prior to making more definitive conclusions and preparing management strategies.

4.6 Conclusions

Local thermal conditions seem to drive thermal tolerance across reefs of the West Indian Ocean. We found strong molecular signals of heat stress adaptation in corals from thermally variable environments, such as at the Rodrigues and Mauritius Islands. The genetic variants potentially implicated in thermal adaptation were associated with genes coding for proteins implemented in heat stress response, notably the heat-shock protein co-chaperone Sacsin. However, large sea distances and strong oceanographic barriers inhibit the genetic exchange of adapted genotypes across the WIO, calling for local-level management of reefs within a framework of a larger regional management plan. Further research into phenotypic expressions of hypothesised target genes will need to be carried out to validate adaptive potentials of corals during stressed conditions. Insights from this research contribute to a growing understanding of coral adaptation to thermal stress that can inform conservation strategies aimed at preserving thermally tolerant genotypes across the WIO in the face of ongoing climate change.

Acknowledgements

This study was conducted with funding provided under the Coral Reef Restoration Project (PIMS 5736) by the Adaptation Fund through United Nations Development Programme Mauritius (sampling permit in Rodrigues SPA 30) and the Government of Seychelles (sampling permit A0157). We gratefully acknowledge the contributions of the following institutions to the field sampling efforts: Albion Fisheries Research Center, Eco Sud, Marine Conservation Society Seychelles, Mauritius Oceanographic Institute, Nature Seychelles, Seychelles National Park Authority, and Shoals Rodrigues. We also thank the United Nations Development Programme of Mauritius for their support in coordinating activities throughout the project.

Data availability statement

Data for this study will soon be made available

Raw DArT sequence data have been deposited in the NCBI BioProject database under accession number PRJNA1277000. Metadata for sampled and genotyped individuals can also be found on GEOME at https://n2t.net/ark:/21547/GQW2

Genotype files, sampling locations, environmental data and scripts used for our analyses will be made available on Dryad.

Conflict of Interest statement

The authors declare no conflict of interests

References

Abelson, A., Nelson, P.A., Edgar, G.J., Shashar, N., Reed, D.C., Belmaker, J., Krause, G., Beck, M.W., Brokovich, E., France, R., Gaines, S.D., 2016. Expanding marine protected areas to include degraded coral reefs. Conserv. Biol. 30, 1182–1191. https://doi.org/10.1111/cobi.12722

Adam, A.A.S., Thomas, L., Underwood, J., Gilmour, J., Richards, Z.T., 2022. Population connectivity and genetic offset in the spawning coral *Acropora digitifera* in Western Australia. Mol. Ecol. 31, 3533–3547. https://doi.org/10.1111/mec.16498

Ainsworth, T.D., Heron, S.F., Ortiz, J.C., Mumby, P.J., Grech, A., Ogawa, D., Eakin, C.M., Leggat, W., 2016. Climate change disables coral bleaching protection on the Great Barrier Reef. Science (80-.). 352, 338–342. https://doi.org/10.1126/science.aac7125

Allen Coral Atlas, 2022. Imagery, maps and monitoring of the world's tropical coral reefs [WWW Document]. https://doi.org/10.5281/zenodo.3833242

Baums, I.B., 2008. A restoration genetics guide for coral reef conservation. Mol. Ecol. 17, 2796–2811. https://doi.org/10.1111/j.1365-294X.2008.03787.x

Bay, R.A., Palumbi, S.R., 2014. Multilocus adaptation associated with heat resistance in reef-building corals. Curr. Biol. 24, 2952–2956. https://doi.org/10.1016/j.cub.2014.10.044

Benestan, L., Quinn, B.K., Maaroufi, H., Laporte, M., Clark, F.K., Greenwood, S.J., Rochette, R., Bernatchez, L., 2016. Seascape genomics provides evidence for thermal adaptation and current-mediated population structure in American lobster (*Homarus americanus*). Mol. Ecol. 25, 5073–5092. https://doi.org/10.1111/mec.13811

Boeckmann, B., Bairoch, A., Apweiler, R., Blatter, M.C., Estreicher, A., Gasteiger, E., Martin, M.J.,

Michoud, K., O'Donovan, C., Phan, I., Pilbout, S., Schneider, M., 2003. The SWISS-PROT protein knowledgebase and its supplement TrEMBL in 2003. Nucleic Acids Res. 31, 365–370. https://doi.org/10.1093/nar/gkg095

Bonin, A., Nicole, F., Pompanon, F., Miaud, C., Taberlet, P., 2007. Population adaptive index: A new method to help measure intraspecific genetic diversity and prioritize populations for conservation. Conserv. Biol. 21, 697–708. https://doi.org/10.1111/j.1523-1739.2007.00685.x

Bozec, Y., Adam, A.A.S., Nava, B.A., Cresswell, A.K., Haller-Bull, V., Iwanaga, T., Lachs, L., Matthews, S.A., McWhorter, J.K., Anthony, K.R.N., Condie, S.A., Halloran, P.R., Ortiz, J.-C., Riginos, C., Mumby, P.J., 2025. A rapidly closing window for coral persistence under global warming. bioRxiv Prepr. https://doi.org/10.1101/2025.01.23.634487

Bridge, T.C.L., Cowman, P.F., Quattrini, A.M., Bonito, V.E., Sinniger, F., Harii, S., Head, C.E.I., Hung, J.Y., Halafihi, T., Rongo, T., Baird, A.H., 2023. A tenuis relationship: traditional taxonomy obscures systematics and biogeography of the '*Acropora tenuis*' (Scleractinia: Acroporidae) species complex. Zool. J. Linn. Soc. 1–24. https://doi.org/10.1093/zoolinnean/zlad062

Bruno, J., Siddon, C., Witman, J., Colin, P., Toscano, M., 2001. El Niño related coral bleaching in Palau, Western Caroline Islands. Coral Reefs 20, 127–136. https://doi.org/10.1007/s003380100151

Burdon, R.H., Gill, V., Evans, C.R., 1990. Active oxygen species and heat shock protein induction, in: Schlesinger, M.J., Santoro, M.G., Garaci, E. (Eds.). Springer Berlin Heidelberg, Berlin, Heidelberg, pp. 19–25.

809 Capblancq, T., Fitzpatrick, M.C., Bay, R.A., Exposito-Alonso, M., Keller, S.R., 2020. Genomic
810 Prediction of (Mal)Adaptation across Current and Future Climatic Landscapes. Annu. Rev.
811 Ecol. Evol. Syst. 51, 245–269. https://doi.org/10.1146/annurev-ecolsys-020720-042553

812 Capblancq, T., Forester, B.R., 2021. Redundancy analysis: A Swiss Army Knife for landscape
813 genomics. Methods Ecol. Evol. 12, 2298–2309. https://doi.org/10.1111/2041-210x.13722

814 Capblancq, T., Luu, K., Blum, M.G.B., Bazin, E., 2018. Evaluation of redundancy analysis to
815 identify signatures of local adaptation. Mol. Ecol. Resour. 18, 1223–1233.
816 https://doi.org/10.1111/1755-0998.12906

817 Carr, M., Kratochwill, C., Daly-Engel, T., Crombie, T., van Woesik, R., 2025. Geographical
818 patterns of intraspecific genetic diversity reflect the adaptive potential of the coral
819 *Pocillopora damicornis* species complex. PLoS One 20, 1–13.
820 https://doi.org/10.1371/journal.pone.0316380

821 Ceder, M.M., Magnusson, K.A., Weman, H.M., Henriksson, K., Andréasson, L., Lindström, T.,
822 Wiggins, O., Lagerström, M.C., 2024. The mRNA expression profile of glycine receptor
823 subunits alpha 1, alpha 2, alpha 4 and beta in female and male mice. Mol. Cell. Neurosci.
824 131. https://doi.org/10.1016/j.mcn.2024.103976

825 Colleoni, F., Wekerle, C., Näslund, J.O., Brandefelt, J., Masina, S., 2016. Constraint on the
826 penultimate glacial maximum Northern Hemisphere ice topography (≈140 kyrs BP). Quat.
827 Sci. Rev. 137, 97–112. https://doi.org/10.1016/j.quascirev.2016.01.024

828 Combosch, D.J., Vollmer, S. V., 2015. Trans-Pacific RAD-Seq population genomics confirms
829 introgressive hybridization in Eastern Pacific *Pocillopora* corals. Mol. Phylogenet. Evol. 88,
830 154–162. https://doi.org/10.1016/j.ympev.2015.03.022

Cooke, G.M., Schlub, T.E., Sherwin, W.B., Ord, T.J., 2016. Understanding the spatial scale of genetic connectivity at sea: Unique insights from a land fish and a meta-analysis. PLoS One 11, 1–25. https://doi.org/10.1371/journal.pone.0150991

Cooke, I., Ying, H., Forêt, S., Bongaerts, P., Strugnell, J.M., Simakov, O., Zhang, J., Field, M.A., Rodriguez-Lanetty, M., Bell, S.C., Bourne, D.G., van Oppen, M.J.H., Ragan, M.A., Miller, D.J., 2020. Genomic signatures in the coral holobiont reveal host adaptations driven by Holocene climate change and reef specific symbionts. Sci. Adv. 6. https://doi.org/10.1126/sciadv.abc6318

Costanza, R., de Groot, R., Sutton, P., van der Ploeg, S., Anderson, S.J., Kubiszewski, I., Farber, S., Turner, R.K., 2014. Changes in the global value of ecosystem services. Glob. Environ. Chang. 26, 152–158. https://doi.org/10.1016/j.gloenvcha.2014.04.002

Cunning, R., Baker, A.C., 2014. Not just who, but how many: The importance of partner abundance in reef coral symbioses. Front. Microbiol. 5, 1–10. https://doi.org/10.3389/fmicb.2014.00400

Cunning, R., Bay, R.A., Gillette, P., Baker, A.C., Traylor-Knowles, N., 2018. Comparative analysis of the *Pocillopora damicornis* genome highlights role of immune system in coral evolution. Sci. Rep. 8, 1–10. https://doi.org/10.1038/s41598-018-34459-8

De Clippele, L.H., Díaz, L.A., Andradi-Brown, D.A., Lazuardi, M.E., Iqbal, M., Zainudin, I.M., Prabuning, D., van Hooidonk, R., Hakim, A., Agung, F., Dermawan, A., Hennige, S.J., 2023. Evaluating annual severe coral bleaching risk for marine protected areas across Indonesia. Mar. Policy 148, 105428. https://doi.org/10.1016/j.marpol.2022.105428

De Mita, S., Thuillet, A.-C., Gay, L., Ahmadi, N., Manel, S., Ronfort, J., Vigouroux, Y., 2013.

853 Detecting selection along environmental gradients: analysis of eight methods and their
854 effectiveness for outbreeding and selfing populations. Mol. Ecol. 22, 1383–1399.
855 https://doi.org/doi:10.1111/mec.12182

856 Dias, M., Ferreira, A., Gouveia, R., Madeira, C., Jogee, N., Cabral, H., Diniz, M., Vinagre, C., 2019.
857 Long-term exposure to increasing temperatures on scleractinian coral fragments reveals
858 oxidative stress. Mar. Environ. Res. 150, 104758.
859 https://doi.org/10.1016/j.marenvres.2019.104758

860 Dixon, G., Davies, S., Aglyamova, G., Meyer, E., Bay, L., Matz, M., 2015. Genomic determinants of
861 coral heat tolerance across latitudes. Science (80-.). 348, 2014–2016.

862 Donovan, M.K., Burkepile, D.E., Kratochwill, C., Shlesinger, T., Sully, S., Oliver, T.A., Hodgson, G.,
863 Freiwald, J., van Woesik, R., 2021. Local conditions magnify coral loss after marine
864 heatwaves. Science (80-.). 372, 977–980. https://doi.org/10.1126/science.abd9464

865 Drury, C., Lirman, D., 2021. Genotype by environment interactions in coral bleaching. Proc. R.
866 Soc. B Biol. Sci. 288. https://doi.org/10.1098/rspb.2021.0177

867 Dziedzic, K.E., Elder, H., Tavalire, H., Meyer, E., 2019. Heritable variation in bleaching responses
868 and its functional genomic basis in reef-building corals (*Orbicella faveolata*). Mol. Ecol. 28,
869 2238–2253. https://doi.org/10.1111/mec.15081

870 E.U. Copernicus Marine Service Information (CMEMS), 2024.
871 OCEANCOLOUR_GLO_BGC_L4_MY_009_104. Mar. Data Store.
872 https://doi.org/10.48670/moi-00281 (Accessed on 03-04-2024)

873 Elder, H., Weis, V.M., Montalvo-Proano, J., Mocellin, V.J.L., Baird, A.H., Meyer, E., Bay, L.K., 2022.
874 Genetic variation in heat tolerance of the coral *Platygyra daedalea* indicates potential for

875 adaptation to ocean warming. Front. Mar. Sci. 9, 1–15.
876 https://doi.org/10.3389/fmars.2022.925845

877 Elma, E., Gullström, M., Yahya, S.A.S., Jouffray, J.B., East, H.K., Nyström, M., 2023. Post-bleaching
878 alterations in coral reef communities. Mar. Pollut. Bull. 186.
879 https://doi.org/10.1016/j.marpolbul.2022.114479

880 Excoffier, L., Hofer, T., Foll, M., 2009. Detecting loci under selection in a hierarchically
881 structured population. Heredity (Edinb). 103, 285–298.
882 https://doi.org/10.1038/hdy.2009.74

883 Forester, B.R., Lasky, J.R., Wagner, H.H., Urban, D.L., 2018. Comparing methods for detecting
884 multilocus adaptation with multivariate genotype–environment associations. Mol. Ecol.
885 27, 2215–2233. https://doi.org/10.1111/mec.14584

886 François, O., Martins, H., Caye, K., Schoville, S.D., 2016. Controlling false discoveries in genome
887 scans for selection. Mol. Ecol. 25, 454–469. https://doi.org/10.1111/mec.13513

888 Frichot, E., François, O., 2015. LEA: An R package for landscape and ecological association
889 studies. Methods Ecol. Evol. 6, 925–929. https://doi.org/10.1111/2041-210X.12382

890 Fuller, Z.L., Mocellin, V.J.L., Morris, L.A., Cantin, N., Shepherd, J., Sarre, L., Peng, J., Liao, Y.,
891 Pickrell, J., Andolfatto, P., Matz, M., Bay, L.K., Przeworski, M., 2020. Population genetics of
892 the coroal *Acropora millepora*: Toward genomic prediction of bleaching, in: Science.
893 https://doi.org/10.1126/science.aba4674

894 Gawroński, P., Pawełkowicz, M., Tofil, K., Uszyński, G., Sharifova, S., Ahluwalia, S., Tyrka, M.,
895 Wędzony, M., Kilian, A., Bolibok-Brągoszewska, H., 2016. DArT markers effectively target
896 gene space in the rye genome. Front. Plant Sci. 7, 1–13.

https://doi.org/10.3389/fpls.2016.01600

Gélin, P., Fauvelot, C., Mehn, V., Bureau, S., Rouzé, H., Magalon, H., 2017. Superclone expansion, long-distance clonal dispersal and local genetic structuring in the coral *Pocillopora damicornis* type β in Reunion Island, South Western Indian Ocean. PLoS One 12, 1–19. https://doi.org/10.1371/journal.pone.0169692

Gélin, P., Pirog, A., Fauvelot, C., Magalon, H., 2018. High genetic differentiation and low connectivity in the coral *Pocillopora damicornis* type β at different spatial scales in the Southwestern Indian Ocean and the Tropical Southwestern Pacific. Mar. Biol. 165. https://doi.org/10.1007/s00227-018-3428-6

Goetze, J.S., Wilson, S., Radford, B., Fisher, R., Langlois, T.J., Monk, J., Knott, N.A., Malcolm, H., Currey-Randall, L.M., Ierodiaconou, D., Harasti, D., Barrett, N., Babcock, R.C., Bosch, N.E., Brock, D., Claudet, J., Clough, J., Fairclough, D. V., Heupel, M.R., Holmes, T.H., Huveneers, C., Jordan, A.R., McLean, D., Meekan, M., Miller, D., Newman, S.J., Rees, M.J., Roberts, K.E., Saunders, B.J., Speed, C.W., Travers, M.J., Treml, E., Whitmarsh, S.K., Wakefield, C.B., Harvey, E.S., 2021. Increased connectivity and depth improve the effectiveness of marine reserves. Glob. Chang. Biol. 27, 3432–3447. https://doi.org/10.1111/gcb.15635

Gollasch, S., 2008. Is ballast water a major dispersal mechanism for marine organisms?, in: Nentwig, W. (Ed.), Biological Invasions. Springer, Berlin, Heidelberg, pp. 49–57. https://doi.org/10.1007/978-3-540-36920-2_4

Gouezo, M., Golbuu, Y., Fabricius, K., Olsudong, D., Mereb, G., Nestor, V., Wolanski, E., Harrison, P., Doropoulos, C., 2019. Drivers of recovery and reassembly of coral reef communities. Proc. R. Soc. B Biol. Sci. 286. https://doi.org/10.1098/rspb.2018.2908

919 Graham, N.A.J., Jennings, S., MacNeil, M.A., Mouillot, D., Wilson, S.K., 2015. Predicting climate-
920 driven regime shifts versus rebound potential in coral reefs. Nature 518, 94–97.
921 https://doi.org/10.1038/nature14140

922 Green, D.G., Bradbury, R.H., Reichelt, R.E., 1987. Patterns of predictability in coral reef
923 community structure. Coral Reefs 6, 27–34. https://doi.org/10.1007/BF00302209

924 Gruber, B., Unmack, P.J., Berry, O.F., Georges, A., 2018. dartr: An R package to facilitate analysis
925 of SNP data generated from reduced representation genome sequencing. Mol. Ecol.
926 Resour. 18, 691–699. https://doi.org/https://doi.org/10.1111/1755-0998.12745

927 Grupstra, C.G.B., Gómez-Corrales, M., Fifer, J.E., Aichelman, H.E., Meyer-Kaiser, K.S., Prada, C.,
928 Davies, S.W., 2024. Integrating cryptic diversity into coral evolution, symbiosis and
929 conservation. Nat. Ecol. Evol. 8, 622–636. https://doi.org/10.1038/s41559-023-02319-y

930 Guest, J.R., Baird, A.H., Maynard, J.A., Muttaqin, E., Edwards, A.J., Campbell, S.J., Yewdall, K.,
931 Affendi, Y.A., Chou, L.M., 2012. Contrasting patterns of coral bleaching susceptibility in
932 2010 suggest an adaptive response to thermal stress. PLoS One 7, 1–8.
933 https://doi.org/10.1371/journal.pone.0033353

934 Hagedorn, M., Page, C.A., O'Neil, K.L., Flores, D.M., Tichy, L., Conn, T., Chamberland, V.F., Lager,
935 C., Zuchowicz, N., Lohr, K., Blackburn, H., Vardi, T., Moore, J., Moore, T., Baums, I.B.,
936 Vermeij, M.J.A., Marhaver, K.L., 2021. Assisted gene flow using cryopreserved sperm in
937 critically endangered coral. Proc. Natl. Acad. Sci. U. S. A. 118, 1–7.
938 https://doi.org/10.1073/pnas.2110559118

939 Helgoe, J., Davy, S.K., Weis, V.M., Rodriguez-Lanetty, M., 2024. Triggers, cascades, and
940 endpoints: connecting the dots of coral bleaching mechanisms. Biol. Rev. 99, 715–752.

https://doi.org/10.1111/brv.13042

Hemond, E.M., Kaluziak, S.T., Vollmer, S. V., 2014. The genetics of colony form and function in Caribbean Acropora corals. BMC Genomics 15, 1–21. https://doi.org/10.1186/1471-2164-15-1133

Herbert, T.D., Peterson, L.C., Lawrence, K.T., Liu, Z., 2010. Tropical ocean temperatures over the past 3.5 million years. Science (80-.). 328, 1530–1534. https://doi.org/10.1126/science.1185435

Hernawan, U.E., van Dijk, K. jent, Kendrick, G.A., Feng, M., Berry, O., Kavazos, C., McMahon, K., 2023. Ocean connectivity and habitat characteristics predict population genetic structure of seagrass in an extreme tropical setting. Ecol. Evol. 13, 1–14. https://doi.org/10.1002/ece3.10257

Hoegh-Guldberg, O., Mumby, P.J., Hooten, A.J., Steneck, R.S., Greenfield, P., Gomez, E., Harvell, C.D., Sale, P.F., Edwards, A.J., Caldeira, K., Knowlton, N., Eakin, C.M., Iglesias-Prieto, R., Muthiga, N., Bradbury, R.H., Dubi, A., Hatziolos, M.E., 2007. Coral reefs under rapid climate change and ocean acidification. Science (80-.). 318, 1737–1742. https://doi.org/10.1126/science.1152509

Howells, E.J., Abrego, D., Liew, Y.J., Burt, J.A., Meyer, E., Aranda, M., 2021. Enhancing the heat tolerance of reef-building corals to future warming. Sci. Adv. 7. https://doi.org/10.1126/sciadv.abg6070

Howells, E.J., Abrego, D., Meyer, E., Kirk, N.L., Burt, J.A., 2016. Host adaptation and unexpected symbiont partners enable reef-building corals to tolerate extreme temperatures. Glob. Chang. Biol. 22, 2702–2714. https://doi.org/10.1111/gcb.13250

Hughes, T.P., Anderson, K.D., Connolly, S.R., Heron, S.F., Kerry, J.T., Lough, J.M., Baird, A.H., Baum, J.K., Berumen, M.L., Bridge, T.C., Claar, D.C., Eakin, C.M., Gilmour, J.P., Graham, N.A.J., Harrison, H., Hobbs, J.A., Hoey, A.S., Hoogenboom, M., Lowe, R.J., Mcculloch, M.T., Pandolfi, J.M., Pratchett, M., Schoepf, V., 2020. Spatial and temporal patterns of mass bleaching of corals in the Anthropocene 83, 80–83.

Hughes, T.P., Barnes, M.L., Bellwood, D.R., Cinner, J.E., Cumming, G.S., Jackson, J.B.C., Kleypas, J., Van De Leemput, I.A., Lough, J.M., Morrison, T.H., Palumbi, S.R., Van Nes, E.H., Scheffer, M., 2017a. Coral reefs in the Anthropocene. Nature 546, 82–90. https://doi.org/10.1038/nature22901

Hughes, T.P., Kerry, J.T., Álvarez-Noriega, M., Álvarez-Romero, J.G., Anderson, K.D., Baird, A.H., Babcock, R.C., Beger, M., Bellwood, D.R., Berkelmans, R., Bridge, T.C., Butler, I.R., Byrne, M., Cantin, N.E., Comeau, S., Connolly, S.R., Cumming, G.S., Dalton, S.J., Diaz-Pulido, G., Eakin, C.M., Figueira, W.F., Gilmour, J.P., Harrison, H.B., Heron, S.F., Hoey, A.S., Hobbs, J.P.A., Hoogenboom, M.O., Kennedy, E. V., Kuo, C.Y., Lough, J.M., Lowe, R.J., Liu, G., McCulloch, M.T., Malcolm, H.A., McWilliam, M.J., Pandolfi, J.M., Pears, R.J., Pratchett, M.S., Schoepf, V., Simpson, T., Skirving, W.J., Sommer, B., Torda, G., Wachenfeld, D.R., Willis, B.L., Wilson, S.K., 2017b. Global warming and recurrent mass bleaching of corals. Nature 543, 373–377. https://doi.org/10.1038/nature21707

Hughes, T.P., Kerry, J.T., Connolly, S.R., Baird, A.H., Eakin, C.M., Heron, S.F., Hoey, A.S., Hoogenboom, M.O., Jacobson, M., Liu, G., Pratchett, M.S., Skirving, W., Torda, G., 2019. Ecological memory modifies the cumulative impact of recurrent climate extremes. Nat. Clim. Chang. 9, 40–43. https://doi.org/10.1038/s41558-018-0351-2

Humanes, A., Lachs, L., Beauchamp, E.A., Bythell, C., Edwards, A.J., Golbuu, Y., Martinez, H.M.,

986 Palmowski, P., Treumann, A., Steeg, E. Van Der, Hooidonk, R. Van, Guest, J.R., 2022. Within-
987 population variability in coral heat tolerance indicates climate adaptation potential. Proc.
988 R. Soc. B Biol. Sci. 289, 20220872.

989 Jin, Y.K., Lundgren, P., Lutz, A., Raina, J.B., Howells, E.J., Paley, A.S., Willis, B.L., Van Oppen, M.J.H.,
990 2016. Genetic markers for antioxidant capacity in a reef-building coral. Sci. Adv. 2.
991 https://doi.org/10.1126/sciadv.1500842

992 Johnston, E.C., Forsman, Z.H., Flot, J.F., Schmidt-Roach, S., Pinzón, J.H., Knapp, I.S.S., Toonen, R.J.,
993 2017. A genomic glance through the fog of plasticity and diversification in *Pocillopora*. Sci.
994 Rep. 7, 1–11. https://doi.org/10.1038/s41598-017-06085-3

995 Johnston, E.C., Wyatt, A.S.J., Leichter, J.J., Burgess, S.C., 2021. Niche differences in co-occurring
996 cryptic coral species (*Pocillopora* spp.). Coral Reefs. https://doi.org/10.1007/s00338-021-
997 02107-9

998 Kilian, A., Wenzl, P., Huttner, E., Carling, J., Xia, L., Blois, H., Caig, V., Heller-Uszynska, K., Jaccoud,
999 D., Hopper, C., Aschenbrenner-Kilian, M., Evers, M., Peng, K., Cayla, C., Hok, P., Uszynski, G.,
1000 2012. Diversity arrays technology: a generic genome profiling technology on open
1001 platforms. Methods Mol. Biol. 888, 67–89. https://doi.org/10.1007/978-1-61779-870-2_5

1002 Kirk, N.L., Howells, E.J., Abrego, D., Burt, J.A., Meyer, E., 2018. Genomic and transcriptomic
1003 signals of thermal tolerance in heat-tolerant corals (*Platygyra daedalea*) of the
1004 Arabian/Persian Gulf. Mol. Ecol. 27, 5180–5194. https://doi.org/10.1111/mec.14934

1005 Koo, I.C., Ohol, Y.M., Wu, P., Morisaki, J.H., Cox, J.S., Brown, E.J., 2008. Role for lysosomal enzyme
1006 β-hexosaminidase in the control of mycobacteria infection. Proc. Natl. Acad. Sci. U. S. A.
1007 105, 710–715. https://doi.org/10.1073/pnas.0708110105

1008 Krueck, N.C., Treml, E.A., Innes, D.J., Ovenden, J.R., 2020. Ocean currents and the population
1009 genetic signature of fish migrations. Ecology 101, 1–13. https://doi.org/10.1002/ecy.2967

1010 Kusumoto, B., Costello, M.J., Kubota, Y., Shiono, T., Wei, C.L., Yasuhara, M., Chao, A., 2020. Global
1011 distribution of coral diversity: Biodiversity knowledge gradients related to spatial
1012 resolution. Ecol. Res. 35, 315–326. https://doi.org/10.1111/1440-1703.12096

1013 Lachs, L., Donner, S.D., Mumby, P.J., Bythell, J.C., Humanes, A., East, H.K., Guest, J.R., 2023.
1014 Emergent increase in coral thermal tolerance reduces mass bleaching under climate
1015 change. Nat. Commun. 4939. https://doi.org/10.1038/s41467-023-40601-6

1016 Lasky, J.R., Josephs, E.B., Morris, G.P., 2023. Genotype–environment associations to reveal the
1017 molecular basis of environmental adaptation. Plant Cell 35, 125–138.
1018 https://doi.org/10.1093/plcell/koac267

1019 Littman, R.A., Bourne, D.G., Willis, B.L., 2010. Responses of coral-associated bacterial
1020 communities to heat stress differ with Symbiodinium type on the same coral host. Mol.
1021 Ecol. 19, 1978–1990. https://doi.org/10.1111/j.1365-294X.2010.04620.x

1022 Liu, G., Strong, A.E., Skirving, W., 2003. Remote sensing of sea surface temperatures during
1023 2002 barrier reef coral bleaching. Eos (Washington. DC). 84, 2002–2004.
1024 https://doi.org/10.1029/2003EO150001

1025 Lotterhos, K.E., 2023. The paradox of adaptive trait clines with nonclinal patterns in the
1026 underlying genes. Proc. Natl. Acad. Sci. 120, e2220313120.
1027 https://doi.org/10.1073/pnas.2220313120

1028 Lotterhos, K.E., Whitlock, M.C., 2015. The relative power of genome scans to detect local
1029 adaptation depends on sampling design and statistical method. Mol. Ecol. 24, 1031–1046.

https://doi.org/10.1111/mec.13100

Louis, Y.D., Kaullysing, D., Gopeechund, A., Mattan-Moorgawa, S., Bahorun, T., Dyall, S.D., Bhagooli, R., 2016. In hospite Symbiodinium photophysiology and antioxidant responses in Acropora muricata on a coast-reef scale: implications for variable bleaching patterns. Symbiosis 68, 61–72. https://doi.org/10.1007/s13199-016-0380-4

Loya, Y., Sakai, K., Yamazato, K., Nakano, Y., Sambali, H., Van Woesik, R., 2001. Coral bleaching: The winners and the losers. Ecol. Lett. 4, 122–131. https://doi.org/10.1046/j.1461-0248.2001.00203.x

Lukoschek, V., Riginos, C., Van Oppen, M.J.H., 2016. Congruent patterns of connectivity can inform management for broadcast spawning corals on the Great Barrier Reef. Mol. Ecol. 25, 3065–3080. https://doi.org/10.1111/mec.13649

Lundgren, P., Vera, J.C., Peplow, L., Manel, S., van Oppen, M.J.H., 2013. Genotype-environment correlations in corals from the Great Barrier Reef. BMC Genet. 14. https://doi.org/10.1186/1471-2156-14-9

Luu, K., Bazin, E., Blum, M.G.B., 2017. pcadapt: an R package to perform genome scans for selection based on principal component analysis. Mol. Ecol. Resour. 17, 67–77. https://doi.org/10.1111/1755-0998.12592

Matz, M. V., Treml, E.A., Haller, B.C., 2020. Estimating the potential for coral adaptation to global warming across the Indo-West Pacific. Glob. Chang. Biol. 26, 3473–3481. https://doi.org/10.1111/gcb.15060

Mayfield, A.B., Chen, Y.J., Lu, C.Y., Chen, C.S., 2018. The proteomic response of the reef coral Pocillopora acuta to experimentally elevated temperatures. PLoS One 13, 1–24.

https://doi.org/10.1371/journal.pone.0192001

Ménade, M., Kozlov, G., Trempe, J.F., Pande, H., Shenker, S., Wickremasinghe, S., Li, X., Hojjat, H., Dicaire, M.J., Brais, B., McPherson, P.S., Wong, M.J.H., Young, J.C., Gehring, K., 2018. Structures of ubiquitin-like (Ubl) and Hsp90-like domains of sacsin provide insight into pathological mutations. J. Biol. Chem. 293, 12832–12842. https://doi.org/10.1074/jbc.RA118.003939

Mérot, C., Oomen, R.A., Tigano, A., Wellenreuther, M., 2020. A roadmap for understanding the evolutionary significance of structural genomic variation. Trends Ecol. Evol. 35, 561–572. https://doi.org/10.1016/j.tree.2020.03.002

Mijangos, J.L., Gruber, B., Berry, O., Pacioni, C., Georges, A., 2022. dartR v2: An accessible genetic analysis platform for conservation, ecology and agriculture. Methods Ecol. Evol. 13, 2150–2158. https://doi.org/10.1111/2041-210X.13918

Miller, K.J., Ayre, D.J., 2008. Population structure is not a simple function of reproductive mode and larval type: Insights from tropical corals. J. Anim. Ecol. 77, 713–724. https://doi.org/10.1111/j.1365-2656.2008.01387.x

Moberg, F., Folke, C., 1999. Ecological goods and services of coral reef ecosystems. Ecol. Econ. 29, 215–233. https://doi.org/10.1016/S0921-8009(99)00009-9

Morais, J., Morais, R., Tebbett, S.B., Bellwood, D.R., 2022. On the fate of dead coral colonies. Funct. Ecol. 1–13. https://doi.org/10.1111/1365-2435.14182

Morrow, K.M., Ritson-Williams, R., Ross, C., Liles, M.R., Paul, V.J., 2012. Macroalgal extracts Induce bacterial assemblage shifts and sublethal tissue stress in Caribbean corals. PLoS One 7. https://doi.org/10.1371/journal.pone.0044859

Mumby, P.J., Van Woesik, R., 2014. Consequences of ecological, evolutionary and biogeochemical uncertainty for coral reef responses to climatic stress. Curr. Biol. 24, R413–R423. https://doi.org/10.1016/j.cub.2014.04.029

Mydlarz, L.D., McGinty, E.S., Drew Harvell, C., 2010. What are the physiological and immunological responses of coral to climate warming and disease? J. Exp. Biol. 213, 934–945. https://doi.org/10.1242/jeb.037580

Nakajima, Y., Nishikawa, A., Iguchi, A., Sakai, K., 2010. Gene flow and genetic diversity of a broadcast-spawning coral in northern peripheral populations. PLoS One 5, e11149. https://doi.org/10.1371/journal.pone.0011149

Nikula, R., Spencer, H.G., Waters, J.M., 2013. Passive rafting is a powerful driver of transoceanic gene flow. Biol. Lett. 9. https://doi.org/10.1098/rsbl.2012.0821

Obura, D., 2012. The diversity and biogeography of Western Indian Ocean reef-building corals. PLoS One 7. https://doi.org/10.1371/journal.pone.0045013

Obura, D., Gudka, M., Samoilys, M., Osuka, K., Mbugua, J., Keith, D.A., Porter, S., Roche, R., van Hooidonk, R., Ahamada, S., Araman, A., Karisa, J., Komakoma, J., Madi, M., Ravinia, I., Razafindrainibe, H., Yahya, S., Zivane, F., 2022. Vulnerability to collapse of coral reef ecosystems in the Western Indian Ocean. Nat. Sustain. 5, 104–113. https://doi.org/10.1038/s41893-021-00817-0

Ortiz, J.C., Pears, R.J., Beeden, R., Dryden, J., Wolff, N.H., Gomez Cabrera, M. del C., Mumby, P.J., 2021. Important ecosystem function, low redundancy and high vulnerability: The trifecta argument for protecting the Great Barrier Reef's tabular Acropora. Conserv. Lett. 14, 1–18. https://doi.org/10.1111/conl.12817

Otto, S.P., 2018. Adaptation, speciation and extinction in the Anthropocene. Proc. R. Soc. B Biol. Sci. 285. https://doi.org/10.1098/rspb.2018.2047

Oury, N., Mona, S., Magalon, H., 2024. Same places, same stories? Genomics reveals similar structuring and demographic patterns for four Pocillopora coral species in the southwestern Indian Ocean. J. Biogeogr. 51, 754–768. https://doi.org/10.1111/jbi.14788

Palumbi, S.R., Barshis, D.J., Traylor-Knowles, N., Bay, R.A., 2014. Mechanisms of reef coral resistance to future climate change. Science (80-.). 344, 895–898. https://doi.org/10.1126/science.1251336

Parfitt, D.A., Michael, G.J., Vermeulen, E.G.M., Prodromou, N. V., Webb, T.R., Gallo, J.M., Cheetham, M.E., Nicoll, W.S., Blatch, G.L., Chapple, J.P., 2009. The ataxia protein sacsin is a functional co-chaperone that protects against polyglutamine-expanded ataxin-1. Hum. Mol. Genet. 18, 1556–1565. https://doi.org/10.1093/hmg/ddp067

Phillips, H.E., Tandon, A., Furue, R., Hood, R., Ummenhofer, C.C., Benthuysen, J.A., Menezes, V., Hu, S., Webber, B., Sanchez-Franks, A., Cherian, D., Shroyer, E., Feng, M., Wijesekera, H., Chatterjee, A., Yu, L., Hermes, J., Murtugudde, R., Tozuka, T., Su, D., Singh, A., Centurioni, L., Prakash, S., Wiggert, J., 2021. Progress in understanding of Indian Ocean circulation, variability, air-sea exchange, and impacts on biogeochemistry. Ocean Sci. 17, 1677–1751. https://doi.org/10.5194/os-17-1677-2021

Pittman, S., Yates, K., Bouchet, P., Alvarez-Berastegui, D., Andréfouët, S., Bell, S., Berkström, C., Boström, C., Brown, C., Connolly, R., Devillers, R., Eggleston, D., Gilby, B., Gullström, M., Halpern, B., Hidalgo, M., Holstein, D., Hovel, K., Huettmann, F., Jackson, E., James, W., Kellner, J., Kot, C., Lecours, V., Lepczyk, C., Nagelkerken, I., Nelson, J., Olds, A., Santos, R., Scales, K., Schneider, D., Schilling, H., Simenstad, C., Suthers, I., Treml, E., Wedding, L.,

Yates, P., Young, M., 2021. Seascape ecology: Identifying research priorities for an emerging ocean sustainability science. Mar. Ecol. Prog. Ser. 663, 1–29. https://doi.org/10.3354/meps13661

Pokrovac, I., Pezer, Ž., 2022. Recent advances and current challenges in population genomics of structural variation in animals and plants. Front. Genet. 13, 1–12. https://doi.org/10.3389/fgene.2022.1060898

Poquita-Du, R.C., Huang, D., Todd, P.A., 2024. Genome-wide analysis to uncover how Pocillopora acuta survives the challenging intertidal environment. Sci. Rep. 14, 1–11. https://doi.org/10.1038/s41598-024-59268-0

Prata, K.E., Bongaerts, P., Dwyer, J.M., Ishida, H., Howitt, S.M., Hereward, J.P., Crandall, E.D., Riginos, C., 2024. Some reef-building corals only disperse metres per generation. Proc. R. Soc. B Biol. Sci. 291. https://doi.org/10.1098/rspb.2023.1988

Privé, F., 2021. bigutilsr: Utility functions for large-scale data. R package version 0.3.4.

Privé, F., Luu, K., Vilhjálmsson, B.J., Blum, M.G.B., Rosenberg, M., 2020. Performing highly efficient genome scans for local adaptation with R Package pcadapt Version 4. Mol. Biol. Evol. 37, 2153–2154. https://doi.org/10.1093/molbev/msaa053

Quigley, K.M., Bay, L.K., van Oppen, M.J.H., 2020. Genome-wide SNP analysis reveals an increase in adaptive genetic variation through selective breeding of coral. Mol. Ecol. 29, 2176–2188. https://doi.org/10.1111/mec.15482

R Core Team, 2024. R: A language and environment for statistical computing.

Rellstab, C., Gugerli, F., Eckert, A.J., Hancock, A.M., Holderegger, R., 2015. A practical guide to

environmental association analysis in landscape genomics. Mol. Ecol. 24, 4348–4370. https://doi.org/doi:10.1111/mec.13322

Richier, S., Sabourault, C., Courtiade, J., Zucchini, N., Allemand, D., Furla, P., 2006. Oxidative stress and apoptotic events during thermal stress in the symbiotic sea anemone, Anemonia viridis. FEBS J. 273, 4186–4198. https://doi.org/10.1111/j.1742-4658.2006.05414.x

Richmond, R.H., 1987. Energetic relationships and biogeographical differences among fecundity, growth and reproduction in the reef coral Pocillopora damicornis. Bull. Mar. Sci. 41, 594–604.

Riginos, C., Crandall, E.D., Liggins, L., Bongaerts, P., Treml, E.A., 2016. Navigating the currents of seascape genomics: How spatial analyses can augment population genomic studies. Curr. Zool. 62, 581–601. https://doi.org/10.1093/cz/zow067

Riginos, C., Popovic, I., Meziere, Z., Oliver Garcia, V., Byrne, I., Howitt, S.M., Ishida, H., Bairos-Novak, K.R., Humanes, A., Scharfenstein, H., Richards, T., Briggs, E.J., Clark, V., Lei, C., Khan, M., Prata, K.E., 2024. Cryptic species and hybridisation in corals: challenges and opportunities for conservation and restoration. Peer Community J. https://doi.org/10.24072/pcjournal.492

Roff, G., Doropoulos, C., Rogers, A., Bozec, Y.M., Krueck, N.C., Aurellado, E., Priest, M., Birrell, C., Mumby, P.J., 2016. The Ecological Role of Sharks on Coral Reefs. Trends Ecol. Evol. 31, 395–407. https://doi.org/10.1016/j.tree.2016.02.014

Rose, N.H., Bay, R.A., Morikawa, M.K., Palumbi, S.R., 2018. Polygenic evolution drives species divergence and climate adaptation in corals. Evolution (N. Y). 72, 82–94.

1162 https://doi.org/10.1111/evo.13385

1163 Sansaloni, C., Petroli, C., Jaccoud, D., Carling, J., Detering, F., Grattapaglia, D., Kilian, A., 2011.
1164 Diversity Arrays Technology (DArT) and next-generation sequencing combined: genome-
1165 wide, high throughput, highly informative genotyping for molecular breeding of
1166 Eucalyptus. BMC Proc. 5, P54. https://doi.org/10.1186/1753-6561-5-S7-P54

1167 Schmidt-Roach, S., Miller, K.J., Woolsey, E., Gerlach, G., Baird, A.H., 2012. Broadcast Spawning by
1168 *Pocillopora* Species on the Great Barrier Reef. PLoS One 7, 1–7.
1169 https://doi.org/10.1371/journal.pone.0050847

1170 Schoepf, V., Stat, M., Falter, J.L., McCulloch, M.T., 2015. Limits to the thermal tolerance of corals
1171 adapted to a highly fluctuating, naturally extreme temperature environment. Sci. Rep. 5,
1172 1–14. https://doi.org/10.1038/srep17639

1173 Selkoe, K.A., D'Aloia, C.C., Crandall, E.D., Iacchei, M., Liggins, L., Puritz, J.B., Von Der Heyden, S.,
1174 Toonen, R.J., 2016. A decade of seascape genetics: Contributions to basic and applied
1175 marine connectivity. Mar. Ecol. Prog. Ser. 554, 1–19. https://doi.org/10.3354/meps11792

1176 Selmoni, O., Bay, L.K., Exposito-Alonso, M., Cleves, P.A., 2024. Finding genes and pathways that
1177 underlie coral adaptation. Trends Genet. 1–15. https://doi.org/10.1016/j.tig.2024.01.003

1178 Selmoni, O., Lecellier, G., Berteaux-Lecellier, V., Joost, S., 2023. The Reef Environment
1179 Centralized InFormation System (RECIFS): An integrated geo-environmental database for
1180 coral reef research and conservation. Glob. Ecol. Biogeogr. 32, 622–632.
1181 https://doi.org/10.1111/geb.13657

1182 Selmoni, O., Lecellier, G., Magalon, H., Vigliola, L., Benzoni, F., Peignon, C., Joost, S., Berteaux-
1183 Lecellier, V., 2021. Seascape genomics reveals candidate molecular targets of heat stress

adaptation in three coral species. Mol. Ecol. 30, 1892–1906. https://doi.org/10.1111/mec.15857

Selmoni, O., Rochat, E., Lecellier, G., Berteaux-Lecellier, V., Joost, S., 2020a. Seascape genomics as a new tool to empower coral reef conservation strategies: an example on north-western Pacific *Acropora digitifera*. Evol. Appl. 13, 1923–1938. https://doi.org/10.1111/eva.12944

Selmoni, O., Vajana, E., Guillaume, A.S., Rochat, E., Joost, S., 2020b. Sampling strategy optimization to increase statistical power in landscape genomics: a simulation-based approach. Mol. Ecol. Resour. 20, 154–169. https://doi.org/10.1101/603829

Severance, E.G., Karl, S.A., 2006. Contrasting population genetic structures of sympatric, mass-spawning Caribbean corals. Mar. Biol. 150, 57–68. https://doi.org/10.1007/s00227-006-0332-2

Shlesinger, T., van Woesik, R., 2023. Oceanic differences in coral-bleaching responses to marine heatwaves. Sci. Total Environ. 871, 162113. https://doi.org/10.1016/j.scitotenv.2023.162113

Simillion, C., Liechti, R., Lischer, H.E.L., Ioannidis, V., Bruggmann, R., 2017. Avoiding the pitfalls of gene set enrichment analysis with SetRank. BMC Bioinformatics 18, 1–14. https://doi.org/10.1186/s12859-017-1571-6

Skirving, W., Marsh, B., De La Cour, J., Liu, G., Harris, A., Maturi, E., Geiger, E., Mark Eakin, C., 2020. Coraltemp and the coral reef watch coral bleaching heat stress product suite version 3.1. Remote Sens. 12, 1–10. https://doi.org/10.3390/rs12233856

Smith, E.G., Hazzouri, K.M., Choi, J.Y., Delaney, P., Al-Kharafi, M., Howells, E.J., Aranda, M., Burt, J.A., 2022. Signatures of selection underpinning rapid coral adaptation to the world's

1206 warmest reefs. Sci. Adv. 8, 1–10. https://doi.org/10.1126/sciadv.abl7287

1207 Smith, H.A., Moya, A., Cantin, N.E., van Oppen, M.J.H., Torda, G., 2019. Observations of
1208 simultaneous sperm release and larval planulation suggest reproductive assurance in the
1209 coral Pocillopora acuta. Front. Mar. Sci. 6, 1–6.
1210 https://doi.org/10.3389/fmars.2019.00362

1211 Snead, A.A., Tatarenkov, A., Avise, J.C., Taylor, D.S., Turner, B.J., Marson, K., Earley, R.L., 2023.
1212 Out to sea: ocean currents and patterns of asymmetric gene flow in an intertidal fish
1213 species. Front. Genet. 14, 1–16. https://doi.org/10.3389/fgene.2023.1206543

1214 Souter, D., Planes, S., Wicquart, J., Logan, M., Obura, D., Staub, F., 2021. Status of coral reefs of
1215 the world: 2020 report, Global Coral Reef Monitoring Network (GCRMN) and International
1216 Coral Reef Initiative (ICRI). https://doi.org/10.59387/WOTJ9184

1217 Spalding, M.D., Fox, H.E., Allen, G.R., Davidson, N., Ferdaña, Z.A., Finlayson, M., Halpern, B.S.,
1218 Jorge, M.A., Lombana, A., Lourie, S.A., Martin, K.D., McManus, E., Molnar, J., Recchia, C.A.,
1219 Robertson, J., 2007. Marine ecoregions of the world: A bioregionalization of coastal and
1220 shelf areas. Bioscience 57, 573–583. https://doi.org/10.1641/B570707

1221 Sproles, A.E., Oakley, C.A., Matthews, J.L., Peng, L., Owen, J.G., Grossman, A.R., Weis, V.M., Davy,
1222 S.K., 2019. Proteomics quantifies protein expression changes in a model cnidarian
1223 colonised by a thermally tolerant but suboptimal symbiont. ISME J. 13, 2334–2345.
1224 https://doi.org/10.1038/s41396-019-0437-5

1225 Steane, D.A., Potts, B.M., McLean, E., Prober, S.M., Stock, W.D., Vaillancourt, R.E., Byrne, M., 2014.
1226 Genome-wide scans detect adaptation to aridity in a widespread forest tree species. Mol.
1227 Ecol. 23, 2500–2513. https://doi.org/10.1111/mec.12751

1228 Stefanoudis, P. V., Talma, S., Fassbender, N., Swanborn, D., Ochieng, C.N., Mearns, K., Komakoma,
1229 J.D., Otwoma, L.M., Mbije, N.E., Osuka, K.E., Samoilys, M., Shah, N., Samaai, T., Trotzuk, E.,
1230 Tuda, A., Zivane, F., Wagner, D., Woodall, L.C., 2023. Stakeholder-derived
1231 recommendations and actions to support deep-reef conservation in the Western Indian
1232 Ocean. Conserv. Lett. 16, 1–11. https://doi.org/10.1111/conl.12924

1233 Storey, J.D., Tibshirani, R., 2003. Statistical significance for genomewide studies. Proc. Natl.
1234 Acad. Sci. U. S. A. 100, 9440–9445. https://doi.org/10.1073/pnas.1530509100

1235 Storfer, A., Patton, A., Fraik, A.K., 2018. Navigating the interface between landscape genetics
1236 and landscape genomics. Front. Genet. 9. https://doi.org/10.3389/fgene.2018.00068

1237 Sully, S., Hodgson, G., Woesik, R., 2022. Present and future bright and dark spots for coral reefs
1238 through climate change. Glob. Chang. Biol. 1–14. https://doi.org/10.1111/gcb.16083

1239 Tabitha, S.N., Moses, K.S., Rajan, R., 2021. Observations of synchronized spawning, larval
1240 survival and settlement in corals of the genus Acropora in Lakshadweep, India. Curr. Sci.
1241 121, 133–140. https://doi.org/10.18520/cs/v121/i1/133-140

1242 Thomas, L., Kennington, W.J., Evans, R.D., Kendrick, G.A., Stat, M., 2017. Restricted gene flow
1243 and local adaptation highlight the vulnerability of high-latitude reefs to rapid
1244 environmental change. Glob. Chang. Biol. 23, 2197–2205.
1245 https://doi.org/10.1111/gcb.13639

1246 Thomas, L., Underwood, J.N., Rose, N.H., Fuller, Z.L., Richards, Z.T., Dugal, L., Grimaldi, C.M.,
1247 Cooke, I.R., Palumbi, S.R., Gilmour, J.P., 2022. Spatially varying selection between habitats
1248 drives physiological shifts and local adaptation in a broadcast spawning coral on a remote
1249 atoll in Western Australia. Sci. Adv. 9185, 1–12.

Thurber, R.V., Willner-Hall, D., Rodriguez-Mueller, B., Desnues, C., Edwards, R.A., Angly, F., Dinsdale, E., Kelly, L., Rohwer, F., 2009. Metagenomic analysis of stressed coral holobionts. Environ. Microbiol. 11, 2148–2163. https://doi.org/10.1111/j.1462-2920.2009.01935.x

van Etten, J., 2017. R Package gdistance: Distances and Routes on Geographical Grids. J. Stat. Softw. 76, 1–21. https://doi.org/0.18637/jss.v076.i13

van Hooidonk, R., Maynard, J., Tamelander, J., Gove, J., Ahmadia, G., Raymundo, L., Williams, G., Heron, S.F., Planes, S., 2016. Local-scale projections of coral reef futures and implications of the Paris Agreement. Sci. Rep. 6, 1–8. https://doi.org/10.1038/srep39666

Van Oppen, M.J.H., Oliver, J.K., Putnam, H.M., Gates, R.D., 2015. Building coral reef resilience through assisted evolution. Proc. Natl. Acad. Sci. U. S. A. 112, 2307–2313. https://doi.org/10.1073/pnas.1422301112

van Woesik, R., Kratochwill, C., 2022. A global coral-bleaching database, 1980–2020. Sci. Data 9, 1–7. https://doi.org/10.1038/s41597-022-01121-y

Villastrigo, A., Orenes-Salazar, V., García-Meseguer, A.J., Mirón-Gatón, J.M., Mourre, B., Millán, A., Velasco, J., 2023. Oceanic currents maintain the genetic structure of non-marine coastal taxa in the western Mediterranean Sea. npj Biodivers. 2, 1–9. https://doi.org/10.1038/s44185-023-00028-0

Virgen-Urcelay, A., Donner, S.D., 2023. Increase in the extent of mass coral bleaching over the past half-century, based on an updated global database. PLoS One 18, 1–17. https://doi.org/10.1371/journal.pone.0281719

Vogt-Vincent, N.S., Burt, A.J., van der Ven, R.M., Johnson, H.L., 2024. Coral reef potential connectivity in the southwest Indian Ocean. Coral Reefs 43, 1037–1051.

https://doi.org/10.1007/s00338-024-02521-9

Voolstra, C.R., Hume, B.C.C., Armstrong, E.J., Mitushasi, G., Porro, B., Oury, N., Agostini, S., Boissin, E., Poulain, J., Carradec, Q., Paz-García, D.A., Zoccola, D., Magalon, H., Moulin, C., Bourdin, G., Iwankow, G., Romac, S., Banaigs, B., Boss, E., Bowler, C., de Vargas, C., Douville, E., Flores, M., Furla, P., Galand, P.E., Gilson, E., Lombard, F., Pesant, S., Reynaud, S., Sullivan, M.B., Sunagawa, S., Thomas, O.P., Troublé, R., Thurber, R.V., Wincker, P., Planes, S., Allemand, D., Forcioli, D., 2023. Disparate genetic divergence patterns in three corals across a pan-Pacific environmental gradient highlight species-specific adaptation. npj Biodivers. 2, 1–16. https://doi.org/10.1038/s44185-023-00020-8

Ward, S., 1992. Evidence for broadcast spawning as well as brooding in the scleractinian coral *Pocillopora damicornis*. Mar. Biol. 112, 641–646. https://doi.org/10.1007/BF00346182

Weersing, K., Toonen, R.J., 2009. Population genetics, larval dispersal, and connectivity in marine systems. Mar. Ecol. Prog. Ser. 393, 1–12. https://doi.org/10.3354/meps08287

Wellenreuther, M., Mérot, C., Berdan, E., Bernatchez, L., 2019. Going beyond SNPs: the role of structural genomic variants in adaptive evolution and species diversification. Mol. Ecol. 28, 1203–1209. https://doi.org/10.1111/mec.15066

White, C., Selkoe, K.A., Watson, J., Siegel, D.A., Zacherl, D.C., Toonen, R.J., 2010. Ocean currents help explain population genetic structure. Proc. R. Soc. B Biol. Sci. 277, 1685–1694. https://doi.org/10.1098/rspb.2009.2214

Wijayanti, D.P., Indrayanti, E., Wirasatriya, A., Haryanto, A., Haryanti, D., Sembiring, A., Fajrianzah, T.A., Bhagooli, R., 2019. Reproductive seasonality of coral assemblages in the Karimunjawa Archipelago, Indonesia. Front. Mar. Sci. 6, 1–15.

https://doi.org/10.3389/fmars.2019.00195

Yates, K.L., Bouchet, P.J., Caley, M.J., Mengersen, K., Randin, C.F., Parnell, S., Fielding, A.H., Bamford, A.J., Ban, S., Barbosa, A.M., Dormann, C.F., Elith, J., Embling, C.B., Ervin, G.N., Fisher, R., Gould, S., Graf, R.F., Gregr, E.J., Halpin, P.N., Heikkinen, R.K., Heinänen, S., Jones, A.R., Krishnakumar, P.K., Lauria, V., Lozano-Montes, H., Mannocci, L., Mellin, C., Mesgaran, M.B., Moreno-Amat, E., Mormede, S., Novaczek, E., Oppel, S., Ortuño Crespo, G., Peterson, A.T., Rapacciuolo, G., Roberts, J.J., Ross, R.E., Scales, K.L., Schoeman, D., Snelgrove, P., Sundblad, G., Thuiller, W., Torres, L.G., Verbruggen, H., Wang, L., Wenger, S., Whittingham, M.J., Zharikov, Y., Zurell, D., Sequeira, A.M.M., 2018. Outstanding challenges in the transferability of ecological models. Trends Ecol. Evol. 33, 790–802. https://doi.org/10.1016/j.tree.2018.08.001

Yuen, B., Stuart, C.E., Pittman, S.J., Green, S.J., Henderson, L.M., Wedding, L.M., 2023. Habitat suitability models of elkhorn coral provide ecological insight to support coral reef restoration. Restor. Ecol. 31, 1–15. https://doi.org/10.1111/rec.13953

Zhang, X.X., Liu, B.G., Li, Y., Liu, Y., He, Y.X., Qian, Z.H., Li, J.X., 2019. Landscape genetics reveals that adaptive genetic divergence in *Pinus bungeana* (Pinaceae) is driven by environmental variables relating to ecological habitats. BMC Evol. Biol. 19, 1–13. https://doi.org/10.1186/s12862-019-1489-x

Fig. 1. a) Map of the study area in the West Indian Ocean (WIO; map insert, top right) indicating the 15 sampling sites distributed around the Seychelles (Mahé: dark red, Praslin: red), and two of the Mascarene Islands of Mauritius (blue) and Rodrigues (green). Names and site identifiers (S#) used in this study are provided for each reef. The number of genotyped individuals retained after quality filtering are indicated at each sampling site per species, with values first for *Acropora muricata* then *Pocillopora damicornis*. **b)** Environmental characterisation of the study reefs using 10 uncorrelated environmental variables (**Table 1**), where abbreviations are as follows: sSST = standard deviation of sea surface temperature; mDHW = mean degree heating week; HPO = human population density.

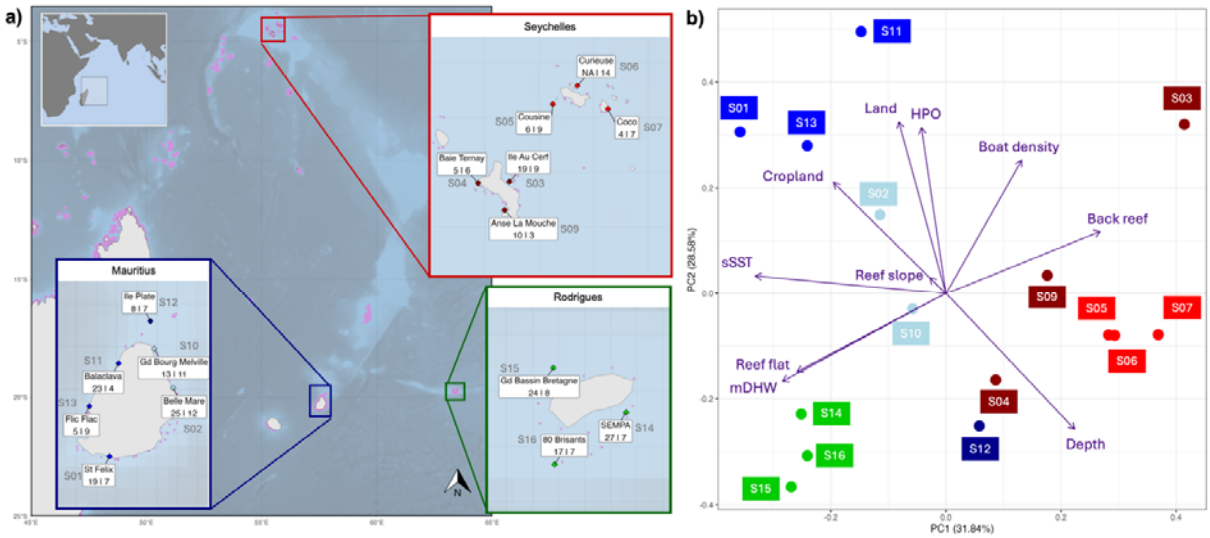

Fig. 2. Population structure analyses of **(A)** *A. muricata* and **(B)** *P. damicornis*, assessed by a principal coordinate analysis (PCoA) and sparse nonnegative matrix factorization (sNMF), with *K*=3 and *K*=4 groups identified for each species respectively in both methods. **i)** Individual scores on PCoA axes 1 and 2 grouped by geographic location (shapes indicate reef and colours indicate subregion; left) and hierarchical cluster grouping of PCoA results (coloured by assigned grouping; right). **ii)** Maps indicating the proportion of individuals at each sampled reef allocated to *K* ancestral populations using sNMF admixture models, where pie chart size indicates the relative number of sampled individuals at each reef and coloured boxes indicate sub-regions. **iii)** Proportion of sampled individuals (columns) allocated to *K* ancestral populations using sNMF admixture models, with individuals grouped by sub-region. Sub region abbreviations: PRA = Praslin, MAH = Mahé, IPL = Ile Plate, MW = West Mauritius, ME = East Mauritius, ROD = Rodrigues.

(A)

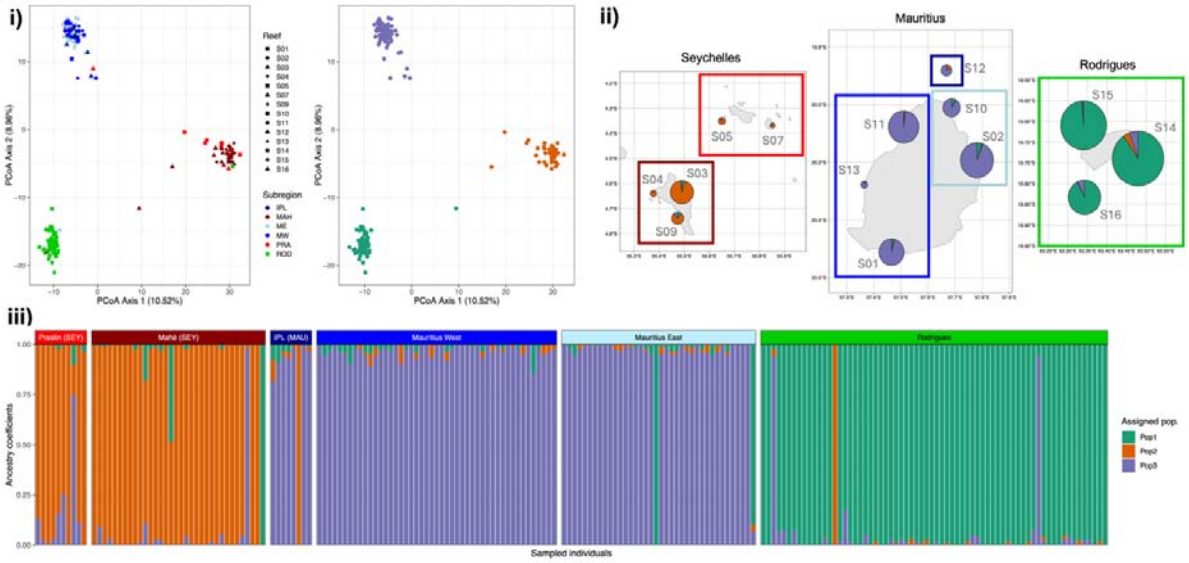

(B)

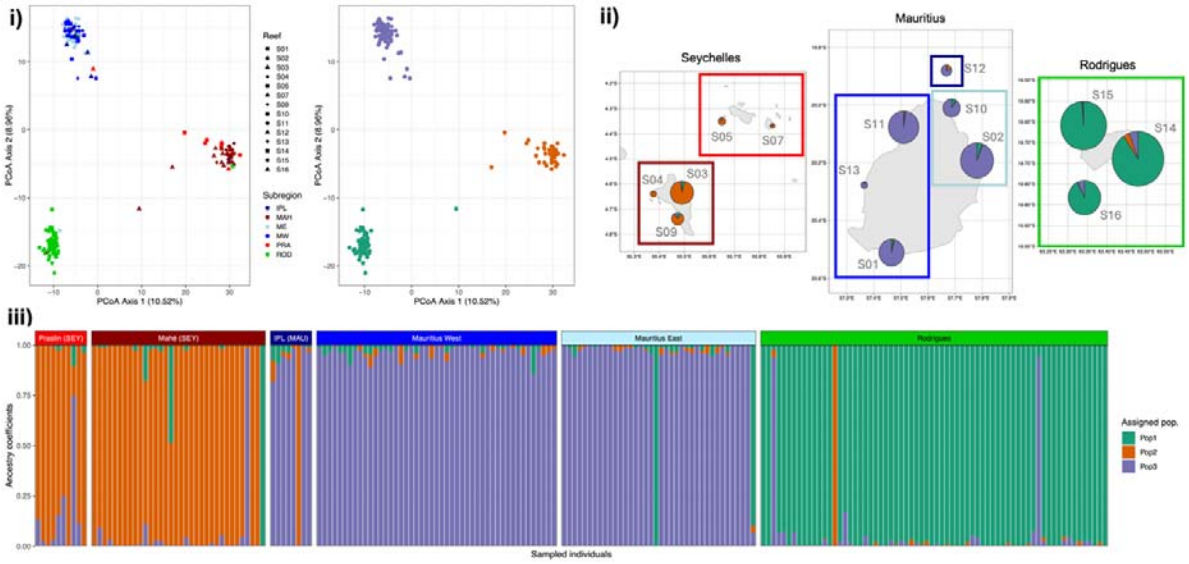
i)
Reef
S01
S02
S03
S04
S05
S07
S09
S10
S11
S12
S13
S14
S15
S16
Subregion
IPL
MAH
ME
MW
PRA
ROD
PCoA Axis 1 (10.52%)
PCoA Axis 2 (8.96%)
ii)
Seychelles
Mauritius
Rodrigues
S01
S02
S03
S04
S05
S07
S09
S10
S11
S12
S13
S14
S15
S16
iii)
Praslin (SEY)
Mahé (SEY)
IPL (MAU)
Mauritius West
Mauritius East
Rodrigues
Ancestry coefficients
Sampled individuals
Assigned pop.
Pop1
Pop2
Pop3

1339

Fig. 3. Adaptive potential indices and predictive sea currents for **(A)** *A. muricata* and **(B)** *P. damicornis*. **i)** Connectivity model performance boxplots, measured as R^2, for models describing the relationship between $\log_{10}$ of the genetic distance (F_{ST}) and $\log_{10}$ of the geographic distance, where boxplots show the spread of R^2 values of connectivity models built with leave-one-reef-out jackknife analyses, assessing the Euclidean geographic distance ('geo') and sea current averaged over each month (01–12) and the year (13). **ii)** Log_{10}-$\log_{10}$ relationship between the genetic distance (F_{ST}) and sea distance obtained from the strongest connectivity predictor (December sea currents for *A. muricata* in **(A)**; annual sea currents for *P. damicornis* in **(B)**). The blue dotted lines indicate the sea distance that corresponds to F_{ST}=0.1. **iii)** Adaptive Potential Index (API in km^2) across the whole WIO region, calculated by combining Inbound Connectivity and Adaptive Scores. Larger API indicates more probability of hosting adaptive genotypes up-current of connected reefs. Arrows indicate sea current velocity of the strongest connectivity predictor.

(A)

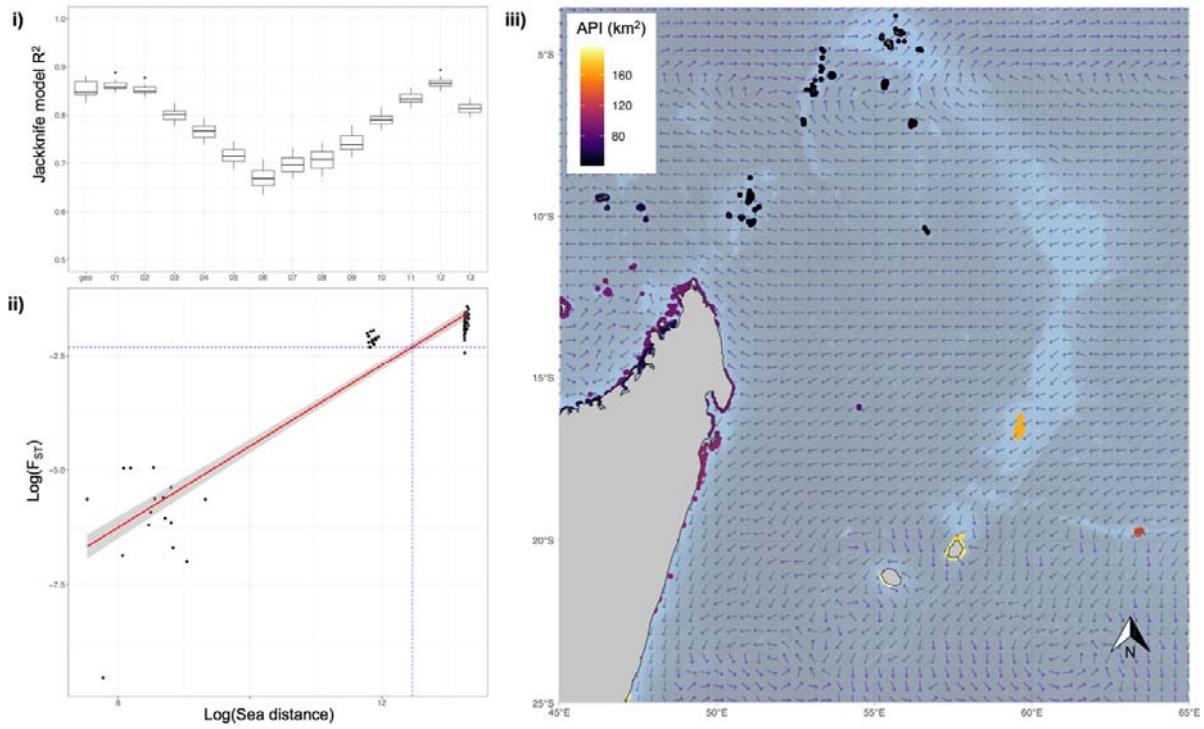

(B)

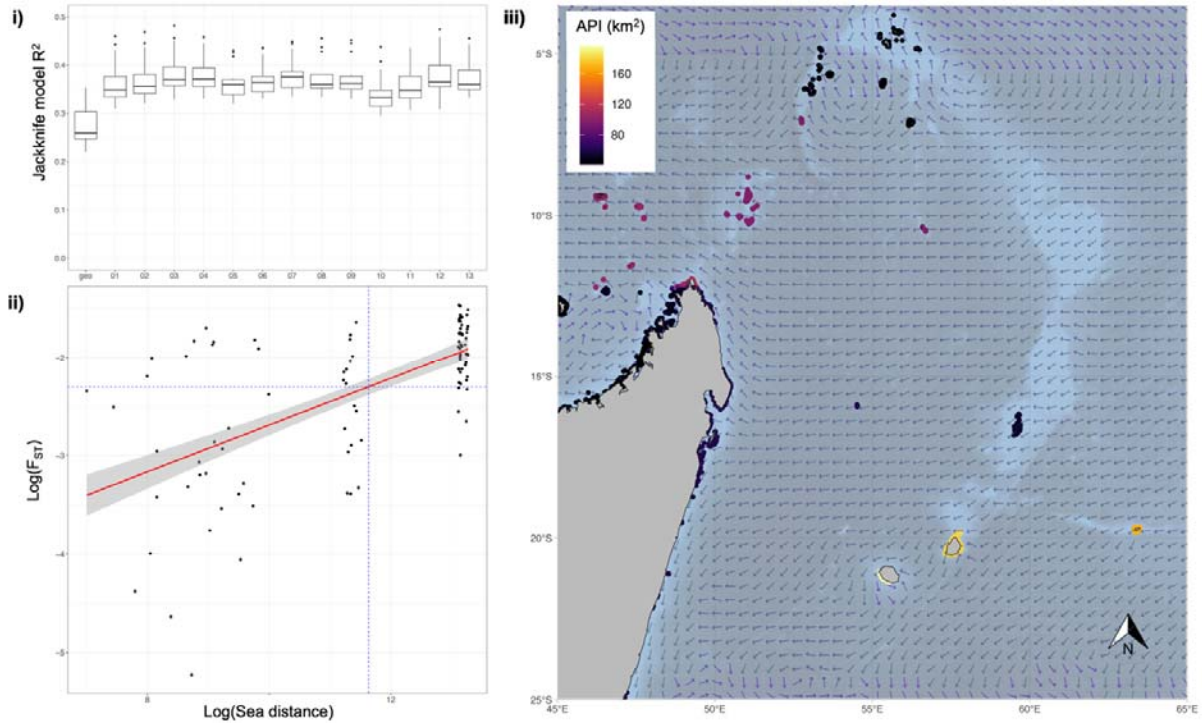

Fig. 4. Genotype–environment association results for **(A)** *A. muricata* and **(B)** *P. damicornis*, using multivariate partial RDA (redundancy analyses) at the reef-level. **i)** RDA biplots projecting loci (dots) and environmental variables (arrows, where sSST is the standard deviation of sea surface temperature and mDHW is the mean of the degree heating weeks). Locus scores are rescaled by a factor of 12 to improve visibility. **ii)** Manhattan plots with the distribution of −log10(q-values) in the genomes. For the first two panels, loci that were identified as outliers (q-value<0.05) are coloured in orange, where outlier loci found within ±10kbp of significantly enriched genes (determined using SetRank) are labelled as diamonds and colour-coded by protein function. **iii)** Tables summarising the significantly enriched gene ontology (GO) terms and their associated protein names and descriptions, alongside SetRank results and the associated genes. Protein names and GO terms are colour coded to match panels **i)** and **ii)**.

(A)

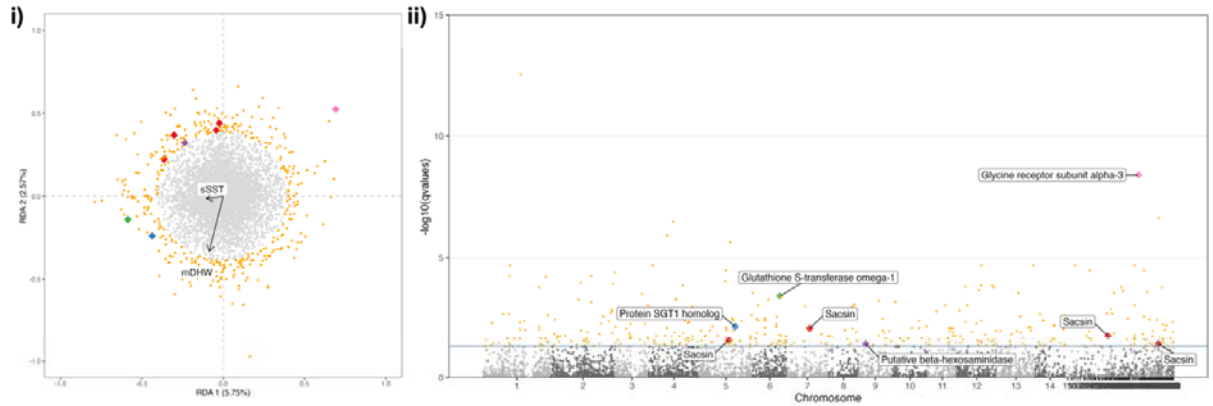

iii)

Protein name	GO Term	Description	Size	setRank	pSetRank	Corrected *P*-value	Adjusted *P*-value	Gene count	Associated significant genes
Glycine receptor subunit alpha-3	GO:0022852	glycine-gated chloride ion channel activity	4	0.0058	1	<0.001	0.0001	2	LOC114961419, LOC122953186
Putative beta-hexosaminidase (EC 3.2.1.52)	GO:0030247	polysaccharide binding	5	0.0058	1	<0.001	0.0038	4	LOC114970115, LOC122962684, LOC114970113, LOC122962769
	GO:0004563	beta-N-acetylhexosaminidase activity	6	0.0108	1	<0.001	0.0038	4	LOC114970115, LOC122962684, LOC114970113, LOC122962769
Protein SGT1 homolog (Protein 40-6-3) (Sgt1) (Suppressor of G2 allele of SKP1 homolog); Sacsin (DNAJC29)	GO:0051087	chaperone binding	28	0.0083	1	0.001	0.0052	6	LOC114966986, LOC114969938, LOC114962707, LOC122954437, LOC114955677, LOC114969949
Sacsin (DNAJC29)	GO:0070628	proteasome binding	11	0.0058	1	<0.001	0.0052	5	LOC114966986, LOC114969938, LOC114962707, LOC122954437, LOC114969949
	GO:0030544	Hsp70 protein binding	24	0.0154	1	0.001	0.0052	5	LOC114966986, LOC114969938, LOC114962707, LOC122954437, LOC114969949
Glutathione S-transferase omega-1 (GSTO-1) (EC 2.5.1.18)	GO:0045174	glutathione dehydrogenase (ascorbate) activity	2	0.0058	1	<0.001	0.0094	2	LOC114959732, LOC114959681

(B)

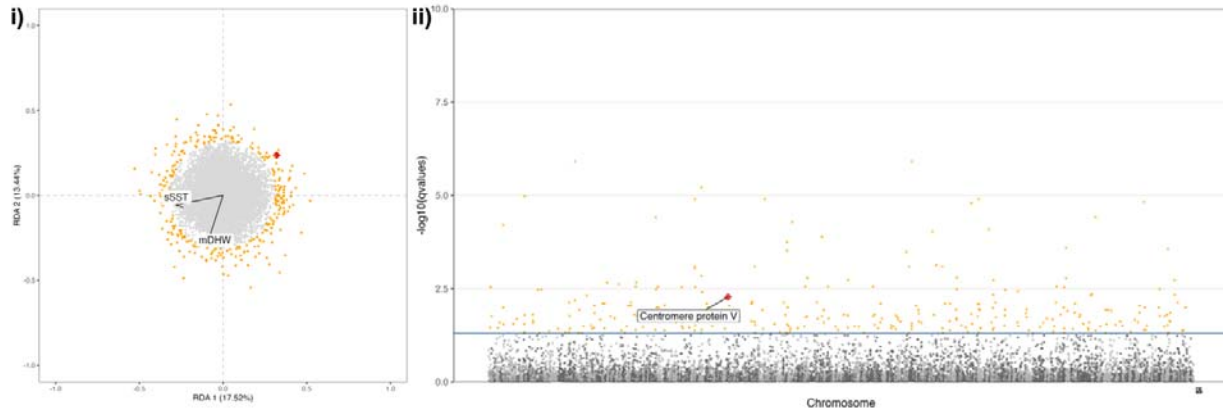

iii)

Protein name	GO Term	Description	Size	setRank	pSetRank	Corrected *P*-value	Adjusted *P*-value	Gene count	Associated significant genes
Centromere protein V (CENP-V) Proline-rich protein 6 and Nuclear protein p30	GO:0016846	carbon-sulfur lyase activity	5	0.0065	1	<0.001	<0.001	4	LOC113669560, LOC113669559, LOC113669558, LOC113669556

1363

Table 1. Summary of the uncorrelated environmental variables used to characterise the seascape of 15 reefs sampled for this research.

Variable	Acronym	Source	Spatial resolution	Temporal resolution
Depth	DEP	RECIFS	5x5 km	n/a
Degree Heating Week (mean)	mDHW	RECIFS	5x5 km	Monthly max from 1985–2021
Sea Surface Temperature (standard deviation)	sSST	RECIFS	5x5 km	Monthly max from 1985–2021
Density of cropland	CROP	RECIFS	5x5 km	Measured in 2015–2019
Density of land	LAND	RECIFS	5x5 km	n/a
Human population along coastline	HPOP	RECIFS	5x5 km	Measured in 2000, 2005, 2010, 2015, 2020
Boat detection	BOAT	RECIFS	5x5 km	Measured in 2017-2021
Fraction of reef slope in 250m around reef	ReefSlope	ACA	10x10 m	n/a
Fraction of reef flat in 250m around reef	ReefFlat	ACA	10x10 m	n/a
Fraction of back reef in 250m around reef	BackReef	ACA	10x10 m	n/a

Table 2. Pairwise F_{ST} between study sites for *A. muricata* (lower triangle) and *P. damicornis* (upper triangle) based on neutral SNP genotype matrices. Sites are grouped and coloured by region and subregion. F_{ST} >0.20 are highlighted in yellow.

Pocillopora damicornis

Acropora muricata			Seychelles						Mauritius						Rodrigues		
			PRA			MAH			IPL	MW			ME		ROD		
			S06	S05	S07	S03	S04	S09	S12	S01	S11	S13	S02	S10	S14	S15	S16
Seychelles	PRA	S06		0.02	0.11	0.03	0.03	0.04	0.15	0.14	0.12	0.17	0.15	0.16	0.13	0.15	0.16
		S05	–		0.06	0.05	0.02	0.07	0.12	0.10	0.10	0.20	0.17	0.17	0.11	0.14	0.14
		S07	–	0.00		0.16	0.09	0.15	0.08	0.05	0.10	0.23	0.21	0.20	0.07	0.13	0.10
	MAH	S03	–	0.00	0.01		0.05	0.10	0.20	0.19	0.17	0.23	0.20	0.21	0.18	0.21	0.22
		S04	–	0.00	0.01	0.00		0.08	0.14	0.12	0.12	0.20	0.17	0.17	0.11	0.14	0.14
		S09	–	0.00	-0.02	0.00	0.00		0.15	0.15	0.13	0.20	0.17	0.18	0.14	0.17	0.19
Mauritius	IPL	S12	–	0.12	0.09	0.14	0.15	0.09		-0.01	0.01	0.15	0.14	0.13	0.03	0.07	0.06
	MW	S01	–	0.18	0.15	0.20	0.21	0.15	0.00		0.04	0.18	0.16	0.16	0.04	0.08	0.06
		S11	–	0.17	0.15	0.19	0.21	0.14	0.00	0.00		0.03	0.05	0.04	0.03	0.05	0.08
		S13	–	0.16	0.13	0.18	0.20	0.12	-0.01	0.00	0.00		0.03	0.02	0.14	0.13	0.19
	ME	S02	–	0.17	0.16	0.19	0.21	0.14	0.01	0.00	0.00	0.00		0.01	0.10	0.11	0.16
		S10	–	0.17	0.14	0.18	0.20	0.13	0.00	0.00	0.00	-0.01	0.00		0.12	0.12	0.17
Rodrigues	ROD	S14	–	0.19	0.17	0.19	0.22	0.15	0.10	0.12	0.12	0.11	0.11	0.10		0.01	-0.01
		S15	–	0.21	0.20	0.21	0.24	0.17	0.13	0.14	0.14	0.14	0.13	0.13	0.00		0.04
		S16	–	0.20	0.19	0.21	0.23	0.16	0.11	0.12	0.12	0.12	0.11	0.11	0.00	0.00	

Sub-region abbreviations: PRA = Praslin, MAH = Mahé, IPL = Ile Plate, MW = West Mauritius, ME = East Mauritius, ROD = Rodrigues

Table 3. Adaptive potentials and connectivity metrics for *A. muricata* and *P. damicornis* at 15 coral reefs across the West Indian Ocean. The Adaptive Score (AS) indicates the relative level of adaptation to thermal stressors (sSST and mDHW) from 0 to 1 (low to high adaptive values), as determined by a GEA analysis. Inbound and Outbound Connectivity indices (ICI and OCI, respectively) indicate the respective area (in km^2) of reef up-current and down-current that fall within a sea distance corresponding to genetic connectivity of F_{ST}<0.1. The Adaptive Potential Index (API) indicates the area (in km^2) of reefs upstream (ICI) that contain adapted corals (AS>0.8). See **Supp Fig. S5** for spatial representations.

Reef information					***A. muricata***				***P. damicornis***			
Code	**Region**	**Reef Name**	**LON**	**LAT**	**AS**	**ICI**	**OCI**	**API**	**AS**	**ICI**	**OCI**	**API**
S05	SEY	Cousine	55.651	-4.351	0.122	1549.0	935.5	41.1	0.134	850.9	869.4	0.0
S06	SEY	Curieuse	55.740	-4.284	–	–	–	–	0.133	850.9	850.4	0.0
S07	SEY	Coco	55.853	-4.369	0.119	1549.0	935.5	41.1	0.132	811.3	865.5	0.0
S03	SEY	Ile Au Cerf	55.491	-4.635	0.154	1549.0	1342.5	41.1	0.163	869.4	869.4	0.0
S04	SEY	Baie Ternay	55.377	-4.640	0.156	1549.0	1386.7	41.1	0.164	850.9	887.0	0.0
S09	SEY	Anse La Mouche	55.474	-4.739	0.152	1549.0	1386.7	41.1	0.159	869.4	887.0	0.0
S12	MAU	Ile Plate	57.668	-19.881	0.576	697.8	580.3	181.2	0.550	685.6	299.4	102.3

S01	MAU	St Felix	57.465	-20.512	0.604	703.8	509.4	187.2	0.576	680.5	299.4	102.3
S11	MAU	Balaclava	57.510	-20.077	0.438	703.8	494.4	187.2	0.407	685.6	299.8	102.3
S13	MAU	Flic Flac	57.365	-20.277	0.499	703.8	456.5	187.2	0.469	685.6	300.4	102.3
S02	MAU	Belle Mare	57.781	-20.192	0.739	703.8	517.1	187.2	0.716	678.2	299.4	102.3
S10	MAU	Gd Bourg Melville	57.687	-20.010	0.598	697.8	537.7	181.2	0.572	685.6	299.4	102.3
S14	ROD	SEMPA	63.479	-19.739	0.797	150.0	698.8	135.9	0.779	150.0	449.4	93.6
S15	ROD	Gd Bassin Bretagne	63.340	-19.659	0.819	150.0	698.8	135.9	0.801	150.0	449.4	93.6
S16	ROD	80 Brisants	63.342	-19.833	0.828	150.0	697.9	135.9	0.810	150.0	449.4	93.6

Region abbreviations: SEY = Seychelles, MAU = Mauritius, ROD = Rodrigues.